Performance Analysis of a Multi-Hop UCRN With Co-Channel Interference

Jamal Ahmed Hussein, *Student Member, IEEE*, Salama S. Ikki, *Member, IEEE*, Said Boussakta, *Senior Member, IEEE*, Charalampos C. Tsimenidis, *Senior Member, IEEE*, and Jonathon Chambers, *Fellow, IEEE*

***Abstract*— In this paper, the performance of a multi-hop underlay cognitive radio network (UCRN) is thoroughly assessed. The co-existence of a primary transceiver and co-channel interference (CCI) is considered along with an uplink single-input multiple-output system utilizing selection combining and maximal ratio combining techniques at the receiver nodes. First, the equivalent per-hop signal-to-interference-plus-noise ratio (SINR) for the UCRN is formulated. Second, the exact cumulative distribution function (CDF) and the probability distribution function of the per-hop SINR are derived and discussed. Furthermore, approximate expressions exhibiting reduced complexity for the per hop equivalent CDF are derived to provide more insights. From the resulting CDF, the exact outage performance of the CR network is thoroughly assessed. In addition, mathematical formulas are derived for the average error probability and system ergodic capacity. Finally, the derived analytical expressions are validated by presenting numerical and simulation results for different network parameters. The results show that several factors contribute to the degradation of the system performance, namely, the interference power constraint, the primary transmitter power, and the presence of CCI, especially in the case where the CCI increases linearly with the secondary transmission powers.**

***Index Terms*— Cognitive radio, multi-hop, co-channel interference, antenna selection, outage performance, error probability performance, ergodic capacity performance.**

I. Introduction

THE RADIO spectrum is a crucial resource that exists for all wireless communication purposes. Cognitive radio (CR) as a solution technique has been suggested in wireless communication to combat the underutilization of the frequency spectrum, i.e. using the existing frequency spectrum more efficiently, and to increase the data throughput of the users [1]. The CR field has inspired several researchers to investigate its implementation possibilities, advantages and challenges [2]. In a CR network, two kinds of users exist and are named as primary user (PU), also known as licensed user, and secondary user (SU), also known as unlicensed user [1]. The PU refers to the users that have a licence to use a specific frequency spectrum at any time without restrictions. SU refers to the users that can use an intended frequency spectrum but with regulations and some restrictions. To realize the CR network, and based on the arrangements of primary and secondary users, three paradigms have been proposed [1], which are *underlay*, *interweave* and *overlay*. In this work, we focus on an underlay CR paradigm to investigate its performance behaviour.

In an underlay cognitive radio network (UCRN), both PU and SU can broadcast signals at the same time in a specific frequency spectrum [2]. However, the PU is protected by a strict threshold power constraint [1] named as the interference power constraint ($I_{\max}$), which is the maximum allowable interference from the SU transmit node to the PU receiver node. This is a key guarantee for the protection of the quality of service (QoS) of the primary network. On the other hand, this interference power constraint is one of the main obstacles to the performance improvement in a UCRN [1]. It limits the transmission power of the SU transmit nodes, since they might not be able to take full advantage of their transmission power capabilities, which will lead to performance limitation and/or degradation. Thus, employment of a cooperative communication network in an underlay CR scheme could be an effective method for combating the impact of the interference power constraint. As a result, the secondary network can take more advantage of the transmission power range and increase the coverage of the secondary network. Different scenarios of the cooperative network have been thoroughly investigated, (see for example [3], [4] and references therein).

It is well-known that employing a multi-antenna scheme in a wireless communication network has the advantage of improvement in the system performance, such as better spectral and power efficiency [5]. In addition, multi-antenna technology has had a major impact on the next generation standards, such as WiMAX and LTE [5], [6]. As a result, it is important to investigate the impact of employing multi-antennas on the UCRN. There are several techniques that can be used to combine the received signal at the receiver of multi-antenna nodes. For example, two common techniques are selection combining (SC), and maximal ratio

Manuscript received January 7, 2016; revised May 12, 2016 and June 21, 2016; accepted July 5, 2016. Date of publication July 14, 2016; date of current version October 14, 2016. This work was supported in part by Leverhulme Trust under grant VP1- 2012-008, EPSRC under grant number EP/H004637/1 and The Higher Committee for Education Development in Iraq (HCED). Data supporting this publication is openly available under an Open Data Commons Open Database License. Additional metadata are available at: http://dx.doi.org/10.17634/100671-1. Please contact Newcastle Research Data Service at rdm@ncl.ac.uk for access instructions. The associate editor coordinating the review of this paper and approving it for publication was Y. Li.

J. A. Hussein, S. Boussakta, C. C. Tsimenidis, and J. Chambers are with the Communications, Sensors, Signal and Information Processing Research Group, School of Electrical and Electronic Engineering, Newcastle University, Newcastle Upon Tyne NE1 7RU, U.K. (e-mail: j.hussein@ncl.ac.uk; said.boussakta@newcastle.ac.uk; charalampos.tsimenidis@ncl.ac.uk; jonathon.chambers@ncl.ac.uk).

S. S. Ikki is with the Electrical Engineering Department, Lakehead University, Thunder Bay, ON P7B 5E1, Canada (e-mail: sikki@lakeheadu.ca).

Color versions of one or more of the figures in this paper are available online at http://ieeexplore.ieee.org.

Digital Object Identifier 10.1109/TCOMM.2016.2591522

combining (MRC). SC is a technique of choosing the best available link, among the possible links between the transmit and receive nodes, that has the highest instantaneous signal-to-noise-ratio (SNR) [7]. It leads to keeping the benefits of the multi-antenna scheme and reducing the hardware cost [8], [9]. This technique has been widely applied to underlay CR networks [10]. In an MRC technique, all of the antennas will contribute to the construction of the received signal. This leads to an improvement of the overall system performance [11].

Co-channel interference (CCI) is one of the factors that degrades the performance of a communication network. Due to the spectrum sharing in the CR network and the frequency re-use in wireless transmission, this kind of interference could be more predictable. It might come from the adjacent clusters or from other licensed and/or unlicensed users in the same cluster [12]. Therefore, it is important to investigate the impact of such interference on the performance characteristics of an underlay CR network.

A. Related Work

Outage probability has been widely studied for different underlay CR scenarios [13]–[16]. For example, the authors in [15], have thoroughly studied the outage probability performance of a multi-hop decode-and-forward (DF) spectrum sharing network considering multiple antenna at the secondary nodes. The direct link between the secondary source and destination was considered. Then, the performance was investigated using both SC and MRC techniques. In the mentioned work, the primary transmitter interference on the secondary network was ignored. In [17], outage performance was studied for dual-hop multi source and multi-relay UCRN. A relay selection method was used in order to improve the performance characteristic; however, no interference was considered on the secondary network. Huang et al. in [16], investigated the outage performance of a dual-hop DF cognitive radio network under the primary network interference and consideration of the Nakagami-*m* fading channels. Multiple nodes were considered at the secondary destination. Furthermore, SNR and signal-to-interference-plus-noise ratio (SINR) based opportunistic user selection techniques were employed to study the outage performance.

Some works have studied the error probability and/or ergodic capacity performance investigation for various underlay CR networks [18]–[20]. For instance, the bit error rate analysis was carried out for a dual-hop multi relay DF spectrum sharing network in [18]. The relay selection technique was employed to enhance the error probability behaviour for the UCRN. In this analysis, the interference from the primary network was ignored. The authors in [19], have studied the outage and error performance in a multiple relay UCRN. In their analysis, the effect of primary network interference was considered on the secondary network. The outage probability and the ergodic capacity performances have been investigated in [20] for a dual-hop multiple relay DF UCRN. The relay selection method was used to determine the outage performance, based on the N^{th} best one, and a single relay was considered to investigate the capacity performance. In the mentioned work, the impact of the primary transmitter was not considered. The authors in [21] studied the outage performance, bit error rate and capacity performances for a multi-hop spectrum sharing network. The power constraint on the secondary transmit nodes were ignored, in addition, primary network interference was ignored. The authors in [12] have investigated the asymptotic outage and error performance in a dual-hop single antenna UCRN. In this work, the effect of primary network and co-channel interferences have been considered, but the effect of additive white Gaussian noise (AWGN) was ignored. Finally, a comprehensive performance for the dual-hop multi-user underlay CR network was investigated in [22], the impact of co-channel interference has been considered; yet, the impact of primary network interference was not considered on the system performance behaviour of the UCRN.

B. Contribution of This Paper

The majority of the previous works have considered a relatively simplified scenario for the system model; such as, not considering the impact of the primary transmitter, considering a single antenna, considering single and/or dual-hop, and/or only studying outage performance. It is obvious that in the presence of interference, the system model becomes more complicated, and the mathematical tractability more challenging [12]. In addition, most of the previous work has focused on the outage performance only, and other performance metrics, such as the average error probability and the ergodic capacity, have not been considered.

The key contribution of this paper is to demonstrate a thorough understanding of the detailed performance behaviour of a pragmatic underlay cognitive radio network. Therefore, the impact of the primary network interference and CCI on the cognitive radio network are examined in the presence of AWGN. In addition, multi-antenna receiver nodes and multi-hop UCRN are studied. More precisely, we have investigated the outage probability, average error probability and the ergodic capacity of the UCRN. In fact, this work is important, especially to a cognitive radio network designer, to better understand the performance characteristics of a UCRN under realistic conditions considered in the network.

Specifically, the decode-and-forward protocol has been assumed at the relay nodes. First, we construct the exact per-hop equivalent SINR expressions considering both opportunistic antenna selection and the maximum ratio combining techniques. In particular, two possible scenarios for the selection combining techniques are considered; SNR-based and SINR-based antenna selection. Second, the exact per-hop cumulative distribution function (CDF) and the probability distribution function (PDF) are derived and discussed. Subsequently, the outage performance, average bit error probability, and the capacity performance are studied. Finally, several numerical examples have been provided to illustrate the system performance characteristics and to support the correctness of the derived results.

From this study, it can be deduced that considering a multi-hop relay network for a UCRN has the advantage of combating the impact of the interference power constraint.

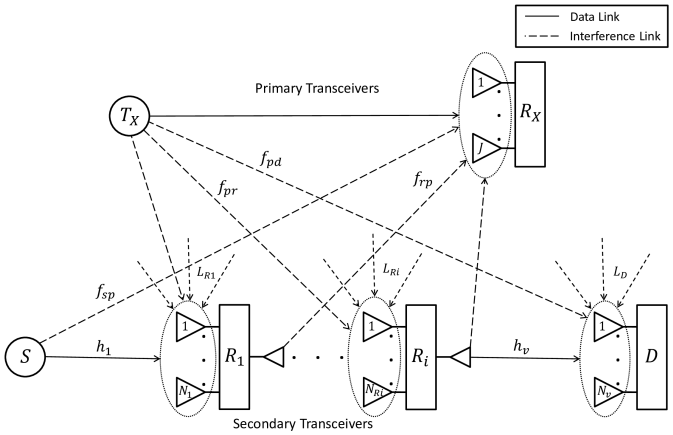

Fig. 1. The general system model used for analysis showing multi-hop underlay CR and primary transceiver networks in the presence of co-channel interference with multi-antennas at all receiver nodes.

It is illustrated that SINR-based antenna selection and MRC consideration provide better performance in comparison to SNR-based antenna selection. However, these approaches require a more complicated hardware configuration and are, hence, practically more challenging. It is also shown that the CCI consideration is severely degrading the performance of the secondary network, especially when its power is considered as linearly increasing with the secondary transmission powers. Furthermore, employing multi-antennas at the receiver nodes can significantly improve the performance and does not lose its importance even in the presence of interferences and $I_{\max}$.

The remainder of this paper is organized as follows. Section II is devoted to the discussion of the system model. Statistical metrics derivations are presented in Section III. Performance analysis metrics are presented and discussed in Section IV. Different numerical and Matlab simulations results are presented and discussed in Section V. The summary and conclusions of this work are given in Section VI. Finally, we give detailed steps of the analytical derivations in Appendices A, B, C, D, and E.

II. System Model

We consider a multi-hop UCRN in which all the nodes in the network have a single transmit antenna and multiple receiver antennas. This system model can be seen as an uplink network, where it is reasonable to assume that the mobile transmitter nodes are equipped with single antennas and the receiver nodes, i.e. base stations are equipped with multiple antennas. The network model is shown in Fig. 1. Specifically, we consider one source node ($S \equiv R_0$), $(V-1)$ relay nodes ($R_i, i = 1, 2, \cdots, V-1$) each with N_{R_i} receive antennas, one destination node ($D \equiv R_V$) with N_D antennas ($N_{D_j}, j = 1, \cdots, N_D$) and a single primary transceiver with J antennas ($J_j, j = 1, \cdots, J$) at the primary receiver node. The nodes in the system operate in half-duplex mode. Relays in the considered system use the decode-and-forward strategy. The fading channels in the multi-hop network are considered as independent, non-identical, Rayleigh fading channels. In addition, we assume that the channels between adjacent transceiver nodes are identical, i.e. the channels between the transmitter and antennas at the receiver side are identical and have the same average channel gains. This is a valid assumption as the distance between the transmitter and either of the corresponding antennas at the receiver node is the same. In our analysis, we define h as the desired channel and f as an interference channel. Let X_{ij_k} represent a generic fading channel coefficient between the i^{th} transmit node and the k^{th} antenna at the j^{th} receiver node in the network, where $k = 1, 2, \cdots, N_j$, and N_j is the number of antennas at the j^{th} receiver node. For example, the channel coefficient between the source and the k^{th} antenna at the first relay node is $h_{SR_{1k}}$. Also, f_{sp_k} is the interference channel coefficient between the secondary source and the k^{th} antenna at the primary receiver, $f_{pr_{R_{1k}}}$ is the interference channel coefficient between the primary source and the k^{th} antenna at the first relay node. Thus, the channel gains are $|X_{ij_k}|^2$ which all follow exponential distributions with mean powers of $\sigma^2_{X_{ij}}$, which can be calculated using $d_{ij}^{-\alpha}$, where d is the distance between the nodes i and j, and α is the path-loss exponent.

In addition, L_{R_i} and L_D are the finite number of co-channel interference signals that affect the R_i relay nodes and the destination node respectively, which are identical in terms of their average energy at the particular secondary receiver nodes. I_{R_i} and I_D are the instantaneous interference-to-noise ratio (INR) that affect each of the R_i relay nodes and the destination node, respectively. Due to the broadcast nature of wireless transmission, these CCI signals could be from any sources in the neighbouring cells or other frequency channels injecting energy into the channel of interest due to non-linear amplifier operation [22]. The fading energies of the individual CCI signals can be modelled as exponential random variables (RVs). Moreover, the sum of the CCI signals at each of the secondary receiver nodes can be modelled by a gamma distributed random variable [23]. In addition, we define $\bar{I}_{R_i}$ and $\bar{I}_D$ as the average CCI powers at the R_i relay nodes and the destination node, respectively. It is worth mentioning that our analyses and results in this work are calculated depending on the average values of the network parameters and not their instantaneous values.

In our analysis, we also consider the transmit power limit from the secondary source nodes; such that each of the secondary transmit nodes has a maximum power constraint P_i, $i = 0, 1, 2, \cdots, V-1$, where P_0 represents the transmit power of the source node. The additive white Gaussian noise, at each of the receiver nodes, is assumed to have zero mean and variance $N_0 \sim \mathcal{CN}(0, N_0)$. In our system model, we assume that the secondary users have exact knowledge of the CSI between the primary user and the secondary users. In an underlay CR scenario, there should be cooperation between the primary user and the secondary user in terms of providing the CSI and the amount of the interference from the secondary user to the primary user. The CSI at the secondary transmitter can be achieved via the feedback link from the primary receiver or through the channel reciprocity [7]. In a multi-antenna scheme, based on the received signal manipulations at the receiver side, there are different methods to obtain the equivalent SINR. In the following sections, two combining

techniques at the secondary receiver nodes are discussed, which are the SC and MRC techniques.

A. Using the SC Technique

In a selection combining technique, the best antenna is selected at the relay and destination nodes, which can be achieved by selecting the highest instantaneous SINR out of $N_{R_{ij}}$ and N_{D_j} antennas at both the R_i and D receiver nodes respectively, at any particular point in time. In terms of simplicity of implementation, SC is considered the simplest combining technique at the receiver side, since only one of the diversity links is used in the process [24, p. 404]. Depending on the antenna selection technique employed at the receiver nodes, there are two possible expressions for the per-hop equivalent instantaneous SINR at each of the receivers:

1) **SNR-based antenna selection:** In this case, only the desired channels between the source and N antennas at the destination are used to pick out the channel which gives the maximum instantaneous SNR. Therefore, the exact instantaneous SINR at the i^{th} hop can be expressed as

$$\gamma_{\text{eq}}^{i} = \frac{\min\left(\frac{I_{\max}}{\max\limits_{k=1,\cdots,J}(|f_{sp_{k_i}}|^2)N_0}, \frac{P_i}{N_0}\right) \max\limits_{n=1,\cdots,N_i}(|h_{n_i}|^2)}{\sum_{j=1}^{L_{R_i}} I_{R_{ij}} + I_{P_{R_i}} + 1}, \tag{1}$$

where $|f_{sp_{k_i}}|^2$ is the channel gain between the secondary transmitter and primary receiver nodes for the i^{th} hop, and $I_{P_{R_i}}$ represent the interference terms from the primary transmitter to the i^{th} hop secondary receiver node.

2) **SINR-based antenna selection:** In this scenario, the interference from the CCI sources and primary network, as well as the noise, are considered in the selection of the best channel. This method is particularly complex practically, since the destination should have complete channel state information (CSI). However, in the first method, the destination does not need that. Thus, the exact i^{th} hop instantaneous SINR for this scenario can be expressed as

$$\gamma_{\text{eq}}^{i} = \min\left(\frac{I_{\max}}{\max\limits_{k=1,\cdots,J}(|f_{sp_{k_i}}|^2)N_0}, \frac{P_i}{N_0}\right) \times \max_{n=1,\cdots,N_i}\left(\frac{|h_{n_i}|^2}{\sum_{j=1}^{L_{R_i}} I_{R_{nij}} + I_{P_{R_{ni}}} + 1}\right). \tag{2}$$

B. Using the MRC Technique

In the MRC technique, all of the antennas at each of the receiver nodes are participating in the resulting SINR. As a result, the exact instantaneous SINR at any i^{th} secondary receiver node can be written as

$$\gamma_{\text{eq}}^{i} = \frac{\min\left(\frac{I_{\max}}{\max\limits_{k=1,\cdots,J}(|f_{sp_{k_i}}|^2)N_0}, \frac{P_i}{N_0}\right) \sum\limits_{n=1}^{N_i}(|h_{n_i}|^2)}{\sum_{j=1}^{L_{R_i}} I_{R_{ij}} + I_{P_{R_i}} + 1}. \tag{3}$$

III. Statistical Analysis

A. Exact Cumulative Distribution Function (CDF)

In order to analyse the characteristics of a random variable, it is important to obtain and inspect its statistical behaviour. In this section, we derive the CDF of the total SINR, known as $\gamma_{\text{eq}}^{\text{tot}}$, for the UCRN. The CDF of a multi-hop DF cooperative network is obtained by [22]

$$F_{\gamma_{\text{eq}}^{\text{tot}}}(\gamma) = 1 - \prod_{i=1}^{V+1}\left(1 - F_{\gamma_{\text{eq}}^{i}}(\gamma)\right). \tag{4}$$

In (4), $F_{\gamma_{\text{eq}}^{i}}(\gamma)$ represents the CDF of the i^{th} hop. In the sections below, we derive the exact CDF of one hop for the scenario of SNR-based antenna selection. The said CDF can be found as follows. Using the formula in (1), the CDF expression of the i^{th} hop SINR can be represented as

$$F_{\gamma_{\text{eq}}^{i}}(\gamma) = \Pr\left(\min\left(\frac{I_{\max}}{W}, P_s\right)\frac{X}{Y+Z+1} \le \gamma\right), \tag{5}$$

where W, X, Y, and Z are representing RVs $\max\limits_{k=1,\cdots,J}(|f_{sp_{k_i}}|^2)$, $\max\limits_{n=1,\cdots,N_i}(|h_{n_i}|^2)$, $\sum_{j=1}^{L_{R_i}} I_{R_{ij}}$, and $I_{P_{R_i}}$ respectively. Since we have assumed the decode-and-forward protocol at the relay nodes, the CDF derivation steps for any particular hop will be similar to the other hops in the network with the condition of using the corresponding per-hop entities to that particular hop. To avoid confusion and make the calculation simpler and more understandable, we use simple representations for the PDF and CDF equation entities, (i.e. we use P_s, σ_h^2, $\sigma_{f_{sp}}^2$, $\bar{I}_R$, $\bar{I}_{P_R}$, N, and L_R instead of P_i, $\sigma_{h_{ij}}^2$, $\sigma_{f_{sp_{ij}}}^2$, $\bar{I}_{R_i}$, $\bar{I}_{P_{R_i}}$, N_i, and L_{R_i} respectively), since these are representing the per-hop entities and for each hop the corresponding entities can be replaced. The PDFs of W, X, Y, and Z are expressed respectively as

$$f_W(w) = \sum_{j=1}^{J}\binom{J}{j}(-1)^{j+1}\frac{j}{\sigma_{f_{sp}}^2}\exp\left(-\frac{wj}{\sigma_{f_{sp}}^2}\right), \tag{6a}$$

$$f_X(x) = \sum_{i=1}^{N}\binom{N}{i}(-1)^{i+1}\left(\frac{i}{\sigma_h^2}\right)\exp\left(-\frac{xi}{\sigma_h^2}\right), \tag{6b}$$

$$f_Y(y) = \frac{y^{L_R-1}}{\bar{I}_R^{L_R}\Gamma(L_R)}\exp\left(-\frac{y}{\bar{I}_R}\right), \tag{6c}$$

$$f_Z(z) = \frac{1}{\bar{I}_{P_R}}\exp\left(-\frac{z}{\bar{I}_{P_R}}\right). \tag{6d}$$

where $\binom{a}{b}$ are the Binomial coefficients defined in [25, eq. (1.2.1)], and can be represented by this formula $\frac{a!}{b!(a-b)!}$.

Proposition 1: The exact CDF of the i^{th} equivalent SINR (i.e. $F_{\gamma_{\text{eq}}^{i}}(\gamma)$) can be written as in (7), as shown at the top of the next page, where Ψ_1 is represented as in (8), as shown at the top of the next page. $E_n(x)$ is the exponential integral function defined in [25, eq. (8.19.2)], and the formula of Ω_n is given as

$$\Omega_n = \frac{1}{(L_R-n)!}\frac{\partial^{L_R-n}}{\partial w^{L_R-n}}\left(\frac{1}{\bar{I}_{P_R}} + w\right)^{-1}\Big|_{w=-\left(\frac{1}{\bar{I}_R}\right)}. \tag{9}$$

$$F_{\gamma_{\text{eq}}^{\text{i}}}(\gamma) = 1 + \sum_{i=1}^{N} \binom{N}{i} (-1)^i \Bigg[\left(\frac{P_s \sigma_h^2}{P_s \sigma_h^2 + i\gamma \bar{I}_{P_R}} \right) \left(\frac{P_s \sigma_h^2}{P_s \sigma_h^2 + i\gamma \bar{I}_R} \right)^{L_R} e^{-\frac{i\gamma}{P_s \sigma_h^2}} \left(1 - e^{-\frac{I_{\max}}{P_s \sigma_{f_{sp}}^2}} \right)^J - \sum_{j=1}^{J} \binom{J}{j} (-1)^j \left(\frac{j I_{\max} \sigma_h^2}{i\gamma \bar{I}_{P_R} \sigma_{f_{sp}}^2} \right) \times \Psi_1 \Bigg], \tag{7}$$

$$\Psi_1 = \begin{cases} \left(\frac{P_s \sigma_h^2}{P_s \sigma_h^2 + i\gamma \bar{I}_R} \right)^{L_R} e^{\frac{j I_{\max} \sigma_h^2 + i\gamma \sigma_{f_{sp}}^2}{i\gamma \bar{I}_R \sigma_{f_{sp}}^2}} E_{L_R+1} \left(\left(\frac{j I_{\max} \sigma_h^2 + i\gamma \sigma_{f_{sp}}^2}{\sigma_{f_{sp}}^2 \sigma_h^2} \right) \left(\frac{P_s \sigma_h^2 + i\gamma \bar{I}_R}{i\gamma \bar{I}_R P_s} \right) \right), & \text{if } \bar{I}_{P_R} = \bar{I}_R \\ \left(\frac{\bar{I}_{P_R}}{\bar{I}_{P_R} - \bar{I}_R} \right)^{L_R} e^{\frac{j I_{\max} \sigma_h^2 + i\gamma \sigma_{f_{sp}}^2}{i\gamma \bar{I}_{P_R} \sigma_{f_{sp}}^2}} E_1 \left(\left(\frac{j I_{\max} \sigma_h^2 + i\gamma \sigma_{f_{sp}}^2}{\sigma_{f_{sp}}^2 \sigma_h^2} \right) \left(\frac{P_s \sigma_h^2 + i\gamma \bar{I}_{P_R}}{i\gamma \bar{I}_{P_R} P_s} \right) \right) \\ + \sum_{n=1}^{L_R} \frac{\Omega_n}{\bar{I}_R^{-L_R}} \left(\frac{P_s \sigma_h^2 \bar{I}_R}{P_s \sigma_h^2 + i\gamma \bar{I}_R} \right)^{n-1} e^{\frac{j I_{\max} \sigma_h^2 + i\gamma \sigma_{f_{sp}}^2}{i\gamma \bar{I}_R \sigma_{f_{sp}}^2}} E_n \left(\left(\frac{j I_{\max} \sigma_h^2 + i\gamma \sigma_{f_{sp}}^2}{\sigma_{f_{sp}}^2 \sigma_h^2} \right) \left(\frac{P_s \sigma_h^2 + i\gamma \bar{I}_R}{i\gamma \bar{I}_R P_s} \right) \right), & \text{otherwise.} \end{cases} \tag{8}$$

Proof: First, we derive the resulting RV from $X/(Y + Z + 1)$. Then, we obtain the exact per-hop unconditional CDF. Let Q represent the new RV resulting from $Y + Z$. To obtain the sum of two random variables, the following formula can be used [26, eq. (6.47)]

$$f_Q(q) = \int_0^q f_Y(y) f_Z(q - y) dy. \tag{10}$$

After substituting $f_Y(y)$, and $f_Z(q-y)$ into the above formula, and with the help of [25, eq. (8.2.1)], we can write the PDF of RV Q as

$$f_Q(q) = \frac{e^{-\frac{q}{\bar{I}_{P_R}}}}{\bar{I}_{P_R} \Gamma(L_R)} \left(\frac{\bar{I}_{P_R}}{\bar{I}_{P_R} - \bar{I}_R} \right)^{L_R} \gamma \left(L_R, \frac{\bar{I}_{P_R} - \bar{I}_R}{\bar{I}_{P_R} \bar{I}_R} q \right), \tag{11}$$

where $\gamma(.,.)$ is the lower incomplete Gamma function. The next step is to obtain the CDF of $\frac{X}{Q+1}$. Let M represent the new RV resulting from $\frac{X}{Q+1}$. To obtain an expression for the CDF of RV M, the following formula can be employed [22]

$$F_M(\gamma) = \int_0^\infty F_X((q+1)\gamma) f_Q(q)\, dq. \tag{12}$$

After substituting $F_X((q + 1)\gamma)$, and $f_Q(q)$ into (12), the resulting integral formula can be solved by employing integration by parts, i.e. $\int u dv = uv - \int v du$, as follows: let $u = \gamma\,(L_R, \varrho_1\, g)$, and $dv = e^{-\varrho_2\, g}$; where $\varrho_1 = \left(\frac{\bar{I}_{P_R} - \bar{I}_R}{\bar{I}_{P_R} \bar{I}_R} \right)$ and $\varrho_2 = \left(\frac{i\gamma \bar{I}_{P_R} + \sigma_h^2}{\sigma_h^2 \bar{I}_{P_R}} \right)$. Therefore, the CDF of the RV M can be written as

$$F_M(\gamma) = 1 - \sum_{i=1}^{N} \binom{N}{i} (-1)^{i+1} e^{-\frac{i\gamma}{\sigma_h^2}} \times \left(\frac{\sigma_h^2}{\sigma_h^2 + i\gamma \bar{I}_{P_R}} \right) \left(\frac{\sigma_h^2}{\sigma_h^2 + i\gamma \bar{I}_R} \right)^{L_R}. \tag{13}$$

Using the total probability theorem, the CDF formula in (5) can be expressed as

$$F_{\gamma_{\text{eq}}^{i}}(\gamma) = \overbrace{\Pr\left(\frac{I_{\max}}{W} M \le \gamma \;,\; \frac{I_{\max}}{W} < P_s \right)}^{I_1} + \overbrace{\Pr\left(P_s M \le \gamma \;,\; \frac{I_{\max}}{W} \ge P_s \right)}^{I_2}. \tag{14}$$

The second part can be directly obtained as follows

$$I_2 = F_M\left(\frac{\gamma}{P_s} \right) F_W\left(\frac{I_{\max}}{P_s} \right). \tag{15}$$

The first part can be represented as

$$I_1 = \int_{\frac{I_{\max}}{P_s}}^{\infty} F_M\left(\frac{\gamma w}{I_{\max}} \right) f_W(w)\, dw. \tag{16}$$

The detailed steps of the solution for the first part (i.e. I_1) are given in Appendix A. Finally, the exact per-hop equivalent CDF can be obtained by combining the derived parts. After some straightforward mathematical arrangements, it can be written as in (7) and (8). Thus, the exact end-to-end CDF expression of $\gamma_{\text{eq}}^{\text{tot}}$ can be obtained by substituting the per-hop derived expressions $F_{\gamma_{\text{eq}}^{i}}(\gamma)$ into (4).

Regarding the per-hop CDF for the case of SINR-based antenna selection, the derivation steps are quite similar to the previous steps, i.e. SNR-based antenna selection. For the sake of saving space, we only provide the final formula expression, which can be written as in (42), and (43), in Appendix B. From the derived CDF expressions of both SNR-based and SINR-based antenna selection techniques, it can be observed that both formulas are relatively similar in terms of mathematical representations. However, in terms of practical aspects, in the SINR-based antenna selection technique, the receiver is required to process all available branches, which is practically challenging. On the other hand, in the SNR-based scenario, only the branch with the highest SNR will participate in the data process detection.

Proposition 2: The exact CDF of the i^{th} equivalent SINR (i.e. $F_{\gamma_{\mathrm{eq}}^{i}}(\gamma)$) for the MRC scenario can be written as

$$F_{\gamma_{\mathrm{eq}}^{\mathrm{i}}}(\gamma) = 1 - \sum_{n=0}^{N-1}\sum_{i=0}^{n}\binom{n}{i}\frac{1}{n!}\frac{1}{\bar{I}_{P_R}}\left(\frac{\bar{I}_{P_R}}{\bar{I}_{P_R}-\bar{I}_R}\right)^{L_R} \times\left[I_{mrc}^{2}-I_{mrc}^{1}\right], \tag{17}$$

where I_{mrc}^{2} and I_{mrc}^{1} are given in (48) and (49) in Appendix C.

Proof: $f_Q(q)$ can be derived, using a similar approach to the previous derivation in Proposition 1, where $Q = Y + Z$. Moreover, in the scenario of the MRC consideration, we should use the following CDF to represent the random variable X [11]

$$F_X(x) = 1 - \sum_{n=0}^{N-1}\frac{1}{n!}e^{-\frac{x}{\sigma_h^2}}\left(\frac{x}{\sigma_h^2}\right)^{n}. \tag{18}$$

In the next step, we substitute $F_X(x)$ and $f_Q(q)$ into (12) to obtain $F_M(\gamma)$. Then, assuming that the number of CCI signals is greater than 1, the resulting integral can be solved as

$$F_M(\gamma) = 1 - \sum_{n=0}^{N-1}\sum_{i=0}^{n}\binom{n}{i}\frac{1}{n!}\frac{1}{\bar{I}_{P_R}}\left(\frac{\bar{I}_{P_R}}{\bar{I}_{P_R}-\bar{I}_R}\right)^{L_R}\left(\frac{\gamma}{\sigma_h^2}\right)^{n} \times e^{\frac{-\gamma}{\sigma_h^2}}\left[\frac{\Gamma(i+1)}{\left(\frac{1}{\bar{I}_{P_R}}+\frac{\gamma}{\sigma_h^2}\right)^{i+1}} - \sum_{m=0}^{L_R-1}(m+1)_i\frac{\left(\frac{\bar{I}_{P_R}-\bar{I}_R}{\bar{I}_{P_R}\bar{I}_R}\right)^{m}}{\left(\frac{1}{\bar{I}_R}+\frac{\gamma}{\sigma_h^2}\right)^{m+i+1}}\right], \tag{19}$$

where $(m+1)_i = \frac{(m+i)!}{m!}$ represents the Pochhammer symbol defined in [25, eq. (5.2.5)]. In the CDF derivation of the MRC case, the scenario where the average INR of the primary transmitter and the CCI sources are not equal is considered, i.e. $\bar{I}_{P_R} \neq \bar{I}_R$. In fact, in the case where $\bar{I}_{P_R} = \bar{I}_R$, the system can be assumed to have $L_R + 1$ interferences at the secondary receiver nodes. The CDF formula for the per hop equivalent SINR in (3) can be expressed in a similar way as in (14). In addition, I_2 can be obtained as in (15), where we should use $F_M(\gamma/P_s)$ that is derived in (19). The derivation steps of I_1 are presented in Appendix C. Therefore, the exact per hop CDF in the MRC case consideration can be obtained by adding both derived parts I_1 and I_2, and can be expressed as in (17).

B. Asymptotic Cumulative Distribution Function (CDF)

The CDF derivation in the previous section gives the exact performance behaviour of the secondary network. However, it does not provide insights about the system parameters. Therefore, in this section, the aim is to present simplified expressions for the per hop equivalent CDF that are less complex in terms of mathematical representation and can give the performance characteristics for a particular network scenario. More specifically, considering the selection combining technique, we study two cases as follows:

Case I ($I_{max} \to \infty$): By employing the condition of $I_{\max} \to \infty$ in (5) and using the formula in (13), we can directly obtain the per hop CDF expression as

$$F_{\gamma_{\mathrm{eq}^{\mathrm{asym-I}}}^{i}}(\gamma) = 1 - \sum_{i=1}^{N}\binom{N}{i}(-1)^{i+1}e^{-\frac{\gamma}{\varpi_1}} \times\left(\frac{\varpi_2}{\varpi_2+\gamma}\right)\left(\frac{\varpi_3}{\varpi_3+\gamma}\right)^{L_R}, \tag{20}$$

where $\varpi_1 = \frac{P_s\sigma_h^2}{i}$, $\varpi_2 = \frac{P_s\sigma_h^2}{i\bar{I}_{P_R}}$, and $\varpi_3 = \frac{P_s\sigma_h^2}{i\bar{I}_R}$. In this scenario, the output CDF is characterized by the transmission power, primary interference power, and the CCI power. However, the interference power constraint does not have any impact on the system performance. This case can be assumed as a special case of an interweave cognitive radio network [1], when the secondary network is broadcasting only in the absence of the primary user.

Case II ($P_s \to \infty$): In this case, when we set $P_s \to \infty$ in (5), it can be observed that the per hop CDF formula can be obtained by taking the expectation of $F_M(\gamma)$ in (13) with respect to the RV W. This can be written mathematically as

$$F_{\gamma_{\mathrm{eq}^{\mathrm{asym-II}}}^{i}}(\gamma) = \int_0^{\infty} F_M\left(\frac{\gamma w}{I_{\max}}\right) f_W(w)\, dw. \tag{21}$$

Assuming only the case where $\bar{I}_{P_R} \neq \bar{I}_R$, the above integral can be solved using similar steps for I_1 in Appendix A, Section B. Therefore, the per hop CDF for case II can be written as

$$F_{\gamma_{\mathrm{eq}^{\mathrm{asym-II}}}^{i}}(\gamma) = 1 - \sum_{i=1}^{N}\sum_{j=1}^{J}\binom{N}{i}\binom{J}{j}(-1)^{j+i}\frac{jI_{\max}}{\sigma_{f_{sp}}^2}\varpi_5\varpi_6^{L_R} \times\left[Ae^{\varpi_4\varpi_5}E_1(\varpi_4\varpi_5) + \sum_{l=1}^{L_R}\frac{B_l}{\varpi_6^{l-1}}e^{\varpi_4\varpi_6}E_l(\varpi_4\varpi_6)\right], \tag{22}$$

where $\varpi_4 = \left(\frac{i\gamma}{\sigma_h^2} + \frac{jI_{\max}}{\sigma_{f_{sp}}^2}\right)$, $\varpi_5 = \left(\frac{\sigma_h^2}{i\gamma\bar{I}_{P_R}}\right)$, and $\varpi_6 = \left(\frac{\sigma_h^2}{i\gamma\bar{I}_R}\right)$. Furthermore, $A = (\varpi_6-\varpi_5)^{L_R}$, and $B_l = \frac{1}{(L_R-l)!}\frac{\partial^{L_R-l}}{\partial w^{L_R-l}}\left(\varpi_5+w\right)^{-1}\Big|_{w=-(\varpi_6)}$. It can be observed that even for the case of unlimited transmission power for the secondary network, the performance behaviour is mainly characterized by the interference power constraint $I_{\max}$. In fact, this $I_{\max}$ is the main obstacle against performance improvement in a UCRN. This scenario is called $I_{\max}$ dominant power transmission.

C. Per-Hop Equivalent Probability Density Function (PDF)

The PDF is another important statistical metric for the equivalent SINR. Knowing this important metric, we can investigate the characteristics and behaviour of the RV, which in our case is the equivalent SINR. The PDF can be obtained

$$f_{\gamma_{\text{eq}}^{\text{i}}}(x) = \sum_{i=1}^{N} \binom{N}{i} (-1)^{i+1} \Bigg[\left(\frac{P_s\sigma_h^2}{i\bar{I}_{P_R}}\right)\left(\frac{P_s\sigma_h^2}{i\bar{I}_R}\right)^{L_R} \left(1 - e^{-\frac{I_{\max}}{P_s\sigma_{f_{sp}}^2}}\right)^{J} \frac{e^{-\frac{xi}{P_s\sigma_h^2}}}{\left(\frac{P_s\sigma_h^2}{i\bar{I}_{P_R}} + x\right)\left(\frac{P_s\sigma_h^2}{i\bar{I}_R} + x\right)^{L_R}} \times \left(\frac{L_R}{\left(\frac{P_s\sigma_h^2}{i\bar{I}_R} + x\right)} + \frac{i}{P_s\sigma_h^2} + \frac{1}{\left(\frac{P_s\sigma_h^2}{i\bar{I}_{P_R}} + x\right)}\right) + \sum_{j=1}^{J} \binom{J}{j} (-1)^{j+1} \left(\frac{jI_{\max}\sigma_h^2}{i\bar{I}_{P_R}\sigma_{f_{sp}}^2}\right) \times \Psi_2 \Bigg], \tag{23}$$

$$\Psi_2 = \begin{cases} \left(\frac{P_s\sigma_h^2}{i\bar{I}_R}\right)^{L_R} \frac{e^{\frac{jI_{\max}\sigma_h^2}{xi\bar{I}_R\sigma_{f_{sp}}^2}}}{x\left(\frac{P_s\sigma_h^2}{i\bar{I}_R}+x\right)^{L_R}} \Bigg\{ \left(\frac{i}{P_s\sigma_h^2} - \frac{jI_{\max}\sigma_h^2}{x^2 i\bar{I}_R\sigma_{f_{sp}}^2}\right) E_{L_R}\left(\frac{jI_{\max}}{P_s\sigma_{f_{sp}}^2} + \frac{xi\sigma_{f_{sp}}^2 + jI_{\max}\sigma_h^2}{xi\bar{I}_R\sigma_{f_{sp}}^2} + \frac{xi}{P_s\sigma_h^2}\right) \\ + \left(\frac{jI_{\max}\sigma_h^2}{x^2 i\bar{I}_R\sigma_{f_{sp}}^2} + \frac{1}{x} + \frac{L_R}{\frac{P_s\sigma_h^2}{i\bar{I}_R}+x}\right) E_{L_R+1}\left(\frac{jI_{\max}}{P_s\sigma_{f_{sp}}^2} + \frac{xi\sigma_{f_{sp}}^2 + jI_{\max}\sigma_h^2}{xi\bar{I}_R\sigma_{f_{sp}}^2} + \frac{xi}{P_s\sigma_h^2}\right) \Bigg\}, & \text{if } \bar{I}_{P_R} = \bar{I}_R \\ \left(\frac{\bar{I}_{P_R}}{\bar{I}_{P_R}-\bar{I}_R}\right)^{L_R} \frac{e^{\frac{1}{\bar{I}_{P_R}}}}{x} \Bigg\{ \frac{1}{x} E_1\left(\frac{jI_{\max}}{P_s\sigma_{f_{sp}}^2} + \frac{1}{\bar{I}_{P_R}} + \frac{jI_{\max}\sigma_h^2}{xi\bar{I}_{P_R}\sigma_{f_{sp}}^2} + \frac{xi}{P_s\sigma_h^2}\right) e^{\frac{jI_{\max}\sigma_h^2}{xi\bar{I}_{P_R}\sigma_{f_{sp}}^2}} \left(\frac{jI_{\max}\sigma_h^2}{xi\bar{I}_{P_R}\sigma_{f_{sp}}^2} + 1\right) \\ + \frac{\left(\frac{i}{P_s\sigma_h^2} - \frac{jI_{\max}\sigma_h^2}{x^2 i\bar{I}_{P_R}\sigma_{f_{sp}}^2}\right) e^{-\frac{xi}{P_s\sigma_h^2}} e^{-\frac{jI_{\max}}{P_s\sigma_{f_{sp}}^2} - \frac{1}{\bar{I}_{P_R}}}}{\left(\frac{jI_{\max}}{P_s\sigma_{f_{sp}}^2} + \frac{1}{\bar{I}_{P_R}} + \frac{jI_{\max}\sigma_h^2}{xi\bar{I}_{P_R}\sigma_{f_{sp}}^2} + \frac{xi}{P_s\sigma_h^2}\right)} \Bigg\} + \sum_{n=1}^{L_R} \frac{\Omega_n e^{\frac{1}{\bar{I}_R}}}{\bar{I}_R^{-L_R}} \left(\frac{P_s\sigma_h^2}{i}\right)^{n-1} \frac{e^{\left(\frac{jI_{\max}\sigma_h^2}{xi\bar{I}_R\sigma_{f_{sp}}^2}\right)}}{x\left(\frac{P_s\sigma_h^2}{i\bar{I}_R}+x\right)^{n}} \\ \Bigg[\left(\frac{P_s\sigma_h^2}{i\bar{I}_R} + x\right)\left(\frac{i}{P_s\sigma_h^2} - \frac{jI_{\max}\sigma_h^2}{x^2 i\bar{I}_R\sigma_{f_{sp}}^2}\right) E_{n-1}\left(\frac{jI_{\max}}{P_s\sigma_{f_{sp}}^2} + \frac{xi\sigma_{f_{sp}}^2 + jI_{\max}\sigma_h^2}{xi\bar{I}_R\sigma_{f_{sp}}^2} + \frac{xi}{P_s\sigma_h^2}\right) \\ + \left(\frac{\left(\frac{jI_{\max}\sigma_h^2}{i\bar{I}_R\sigma_{f_{sp}}^2}\right)\left(\frac{P_s\sigma_h^2}{i\bar{I}_R}+x\right)}{x^2} + \frac{\frac{P_s\sigma_h^2}{i\bar{I}_R}+x}{x} + (n-1)\right) E_n\left(\frac{jI_{\max}}{P_s\sigma_{f_{sp}}^2} + \frac{xi\sigma_{f_{sp}}^2 + jI_{\max}\sigma_h^2}{xi\bar{I}_R\sigma_{f_{sp}}^2} + \frac{xi}{P_s\sigma_h^2}\right) \Bigg], & \text{otherwise.} \end{cases} \tag{24}$$

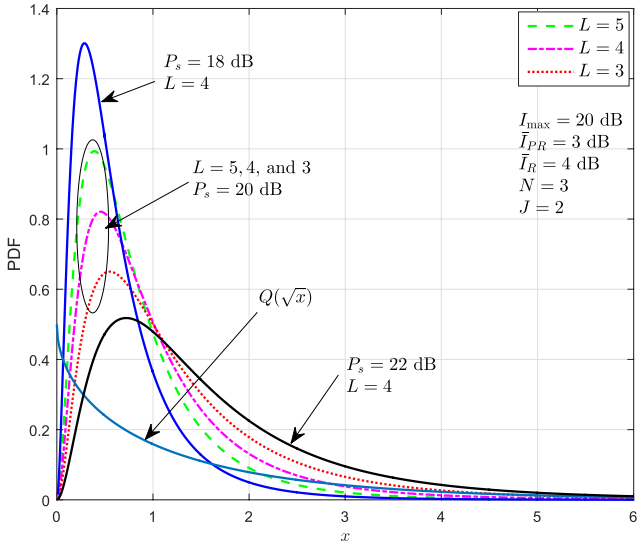

Fig. 2. Characteristics of the PDF of the per-hop equivalent SINR.

by taking the first derivative of the derived CDF with respect to γ. Therefore, the exact per-hop equivalent PDF can be written as in (23), as shown at the top of this page, where Ψ_2 is represented in (24), as shown at the top of this page.

To show the distribution of the calculated equivalent PDF in (23), Fig. 2 has been plotted. The channel variances have been computed based on a two-dimensional network topology scenario, where the secondary source node is located at $(0, 0)$, and its corresponding destination at $(1, 0)$, and the primary destination node is located at $(1, 1)$. In addition, a path-loss exponent of four is assumed. From these plots, we can clearly notice the effect of the CCI signal numbers and transmission power limit P_s. For this analysis, for a fixed value of $I_{\max}$ and different values of the transmission power, we observe that decreasing the value of P_s deteriorates the PDF behaviour, which will lead to degradation of the network performance.

For further clarification about this claim, the function $Q(\sqrt{x})$ has been plotted in Fig. 2. It can be seen that for higher values of x, the behaviour of the PDF gradually becomes insignificant because the Q-function decays to the lowest value, i.e. tends to zero at a higher rate. In this case, the integral is approximately null in most of the integration pattern. However, bearing in mind that $Q(0) = 1/2$, the behaviour of the PDF around the origin is always important. This can be observed in Fig. 2, where as P_s increases, the value of the PDF around zero decreases. Moreover, we have plotted the PDF characteristics for the different number of the CCI signals L. It can be seen that for a higher number of CCI signals the PDF curve becomes closer to the origin, i.e. PDF around zero increases, which means deteriorating the behaviour of the PDF that leads to the degradation of the overall system performance.

IV. Performance Evaluation

A. Outage Probability

The outage probability performance can be easily investigated from the derived end-to-end CDF. It is referred to in the

scenario where the probability of the total calculated SINR of the UCRN is less than or equal to the network predefined SNR threshold γ_{th}. Therefore, the equivalent outage probability for the UCRN can be calculated using the total equivalent CDF that has been derived in the previous section in (4), with the replacement of γ with γ_{th}

$$P_{\text{out}}(\gamma_{\text{th}}) = \Pr\left(\gamma_{\text{eq}}^{\text{tot}} \leq \gamma_{\text{th}}\right) = F_{\gamma_{\text{eq}}^{\text{tot}}}(\gamma_{\text{th}}). \tag{25}$$

B. Average Error Probability

The average bit error probability (ABEP) is one of the important performance criteria for any wireless communication network. The per-hop ABEP could be investigated from the PDF or CDF, i.e. $F^i_{\gamma_{\text{eq}}}(\gamma)$ and $f^i_{\gamma_{\text{eq}}}(x)$ [22]. Yet, it can be observed from the PDF obtained in the previous section that CDF approach could be mathematically more suitable for the calculations, especially in our network model. In particular, we use the CDF that has been derived for the scenario of the SNR-based antenna selection. The ABEP for each hop can be obtained by using the following formula [4]

$$\bar{P}_b^i(e) = \frac{a}{2}\sqrt{\frac{b}{\pi}} \int_0^\infty \frac{\exp(-b\ \gamma)}{\sqrt{\gamma}} F_{\gamma_{\text{eq}}^i}(\gamma)\ d\gamma. \tag{26}$$

In (26), $F_{\gamma_{\text{eq}}^i}(\gamma)$ represents the per-hop equivalent CDF, a and b are constants that depend on the modulation scheme that is used, for instance, QPSK: $a = 2$ and $b = 0.5$ [12]. Moreover, the end-to-end ABEP for a multi-hop decode-and-forward relay protocol can be determined by [21]

$$\bar{P}_b^{e2e}(e) = \sum_{i=1}^{V+1} \bar{P}_b^i(e) \prod_{j=i+1}^{V+1} \left(1 - 2\bar{P}_b^j(e)\right), \tag{27}$$

To obtain the exact per-hop ABEP, we start by substituting the exact derived CDF in (7) and (8) into (26). After solving the equation, the ABEP can be written as in (28)

$$\bar{P}_b^{\text{i}}(e) = \frac{a}{2} + \sum_{i=1}^{N} \binom{N}{i} (-1)^i \frac{a}{2} \begin{cases} \bar{P}_b^I(e), & \text{if } \bar{I}_{P_R} = \bar{I}_R, \\ \bar{P}_b^{II}(e), & \text{otherwise.} \end{cases} \tag{28}$$

where $\bar{P}_b^I(e)$ and $\bar{P}_b^{II}(e)$ have been represented in (29) and (30), as shown at the bottom of this page, which are the first and second case of the ABEP expression, i.e. $\bar{I}_{P_R} = \bar{I}_R$, and $\bar{I}_{P_R} \neq \bar{I}_R$ respectively. $U(a, b, z)$ is the confluent hypergeometric function of the second kind defined in [25, eq. (13.4.4)], and erfc(.) is the complementary error function defined in [25, eq. (7.2.7)]. In addition, μ_{m_1}, and μ_{m_2} are obtained using the formulas given in (31a), and (31b) respectively. Moreover, $I_{P_{b1}}$ and $I_{P_{b2}}$ are determined using (55), and (61) respectively. The derivation steps of the average error probability can be found in Appendix D.

$$\mu_{m_1} = \frac{1}{(L_R - m_1)!} \frac{\partial^{L_R - m_1}}{\partial \gamma^{L_R - m_1}} \left(\frac{P_s\sigma_h^2}{i\bar{I}_{P_R}} + \gamma\right)^{-1}\Bigg|_{\gamma = -\left(\frac{P_s\sigma_h^2}{i\bar{I}_R}\right)} \tag{31a}$$

$$\mu_2 = \left(\frac{P_s\sigma_h^2}{i\bar{I}_R} - \frac{P_s\sigma_h^2}{i\bar{I}_{P_R}}\right)^{-L_R}. \tag{31b}$$

C. Ergodic Capacity

The ergodic capacity is another important measure for any communication system performance; its unit is measured in (bits/second/Hz) [22]. It gives an indication of the possible data rate that the considered network can achieve under some predefined circumstances. In fact, this is important specifically for a cognitive radio network to assess its contribution in providing the amount of data throughput to the intended SU. According to the Shannon theorem for the network capacity measurement, the ergodic capacity can be defined mathematically as the expected value of the instantaneous mutual information between the source and destination. This can be expressed as $C_{erg} \triangleq \text{E}[B\log_2(1 + \gamma_{\text{eq}})]$, where E[.] is the expectation operator, B is the operating bandwidth and γ_{eq} is the total equivalent SNR. Moreover, the ergodic capacity can be obtained using the CDF formula of the total equivalent SINR [22]

$$C_{erg}^i = \int_0^\infty \frac{1}{1+\gamma}\left(1 - F_{\gamma_{\text{eq}}^i}(\gamma)\right)\ d\gamma, \tag{32}$$

$$\bar{P}_b^I(e) = \left(\frac{P_s\sigma_h^2}{i\bar{I}_R}\right)^{L_R+1} \left(1 - e^{-\frac{I_{\max}}{P_s\sigma_{f_{sp}}^2}}\right)^J \sqrt{b}\left(b + \frac{i}{P_s\sigma_h^2}\right)^{L_R+\frac{1}{2}} \text{U}\left(L_R+1, L_R+\frac{3}{2}, \frac{1}{\bar{I}_R}\left(\frac{bP_s\sigma_h^2}{i}+1\right)\right) - \sum_{j=1}^{J}\binom{J}{j}(-1)^j \left(\frac{jI_{\max}\sigma_h^2}{i\bar{I}_R\sigma_{f_{sp}}^2}\right)\left(\frac{P_s\sigma_h^2}{i\bar{I}_R}\right)^{L_R} \sqrt{\frac{b}{\pi}}\ I_{P_{b1}} \tag{29}$$

$$\bar{P}_b^{II}(e) = \left(\frac{P_s\sigma_h^2}{i\bar{I}_{P_R}}\right)\left(\frac{P_s\sigma_h^2}{i\bar{I}_R}\right)^{L_R}\left(1 - e^{-\frac{I_{\max}}{P_s\sigma_{f_{sp}}^2}}\right)^J \times \left[\sqrt{\frac{b\pi i\bar{I}_{P_R}}{P_s\sigma_h^2}}\mu_3 e^{\frac{1}{\bar{I}_{P_R}}\left(\frac{bP_s\sigma_h^2}{i}+1\right)}\text{erfc}\left(\sqrt{\frac{1}{\bar{I}_{P_R}}\left(\frac{bP_s\sigma_h^2}{i}+1\right)}\right) + \sqrt{b}\sum_{m_4=1}^{L_R}\mu_{m_4}\left(b+\frac{i}{P_s\sigma_h^2}\right)^{m_4-\frac{1}{2}} \times \text{U}\left(m_4, m_4+\frac{1}{2}, \frac{1}{\bar{I}_R}\left(\frac{bP_s\sigma_h^2}{i}+1\right)\right)\right] - \sum_{j=1}^{J}\binom{J}{j}(-1)^j\left(\frac{jI_{\max}\sigma_h^2}{i\bar{I}_{P_R}\sigma_{f_{sp}}^2}\right)\sqrt{\frac{b}{\pi}}I_{P_{b2}}. \tag{30}$$

$$C_{erg}^{I} = \left(\frac{P_s\sigma_h^2}{i\bar{I}_R}\right)^{L_R+1}\left(1-e^{-\frac{I_{\max}}{P_s\sigma_{f_{sp}}^2}}\right)^{J}\left(\lambda_1 e^{\frac{i}{P_s\sigma_h^2}}E_1\left(\frac{i}{P_s\sigma_h^2}\right)+\sum_{r_2=1}^{L_R+1}\lambda_{r_2}\left(\frac{P_s\sigma_h^2}{i\bar{I}_R}\right)^{1-r_2}e^{\frac{1}{\bar{I}_R}}E_{r_2}\left(\frac{1}{\bar{I}_R}\right)\right) - \sum_{j=1}^{J}\binom{J}{j}(-1)^j\ \frac{jI_{\max}\sigma_h^2}{i\bar{I}_R\sigma_{f_{sp}}^2}\ \left(\frac{P_s\sigma_h^2}{i\bar{I}_R}\right)^{L_R} I_{C_{erg1}} \tag{35}$$

$$C_{erg}^{II} = \left(\frac{P_s\sigma_h^2}{i\bar{I}_{P_R}}\right)\left(\frac{P_s\sigma_h^2}{i\bar{I}_R}\right)^{L_R}\left(1-e^{-\frac{I_{\max}}{P_s\sigma_{f_{sp}}^2}}\right)^{J}\left(\sum_{r_3=1}^{L_R}\lambda_{r_3}\left(\frac{P_s\sigma_h^2}{i\bar{I}_R}\right)^{1-r_3}e^{\frac{1}{\bar{I}_R}}E_{r_3}\left(\frac{1}{\bar{I}_R}\right) + \lambda_4 e^{\frac{1}{\bar{I}_{P_R}}}E_1\left(\frac{1}{\bar{I}_{P_R}}\right)+\lambda_5 e^{\frac{i}{P_s\sigma_h^2}}E_1\left(\frac{i}{P_s\sigma_h^2}\right)\right) - \sum_{j=1}^{J}\binom{J}{j}(-1)^j\left(\frac{jI_{\max}\sigma_h^2}{i\bar{I}_{P_R}\sigma_{f_{sp}}^2}\right) I_{C_{erg2}} \tag{36}$$

where $F_{\gamma_{\text{eq}}^i}(\gamma)$ represents the CDF of the i^{th} hop of the secondary network. Furthermore, the ergodic capacity for a multi-hop decode-and-forward relay protocol can be calculated as

$$C_{erg}^{e2e} = \min_{i=1,\cdots,V+1}\left(C_{erg}^{i}\right), \tag{33}$$

where C_{erg}^{i} represents the i^{th} hop ergodic capacity of the CR network.

Here, the derivation of the per-hop ergodic capacity is provided. Then, the total system capacity for the UCRN is calculated through replacing the obtained per-hop ergodic capacity from (32) into (33). We start by substituting the per-hop complementary CDF formula into (32). After the evaluation of the integral, the closed-form expression of the per-hop ergodic capacity can be obtained as

$$C_{erg}^{i} = \sum_{i=1}^{N}\binom{N}{i}(-1)^{i+1}\times\begin{cases}C_{erg}^{I}, & \text{if } \bar{I}_{P_R}=\bar{I}_R,\\ C_{erg}^{II}, & \text{otherwise.}\end{cases} \tag{34}$$

where C_{erg}^{I} and C_{erg}^{II} are represented in (35) and (36), as shown at the top of this page, respectively. Furthermore, the entities λ_1, λ_{r_2}, λ_{r_3}, λ_4, and λ_5 are obtained using the formulas given in (37a), (37b), (37c), (37d), and (37e) respectively. Moreover, $I_{C_{erg1}}$ and $I_{C_{erg2}}$ are determined using (66), and (71) respectively. The detailed derivation steps can be found in Appendix E.

$$\lambda_1 = \left(\frac{P_s\sigma_h^2}{i\bar{I}_R}-1\right)^{-(L_R+1)} \tag{37a}$$

$$\lambda_{r_2} = \frac{1}{(L_R+1-r_2)!}\frac{\partial^{L_R+1-r_2}}{\partial\gamma^{L_R+1-r_2}}\left(1+\gamma\right)^{-1}\Big|_{\gamma=-\frac{P_s\sigma_h^2}{i\bar{I}_R}} \tag{37b}$$

$$\lambda_{r_3} = \frac{1}{(L_R-r_3)!}\ \frac{\partial^{L_R-r_3}}{\partial\gamma^{L_R-r_3}}\left(1+\gamma\right)^{-1} \times\left(\frac{P_s\sigma_h^2}{i\bar{I}_{P_R}}+\gamma\right)^{-1}\Big|_{\gamma=-\frac{P_s\sigma_h^2}{i\bar{I}_R}} \tag{37c}$$

$$\lambda_4 = \left(\frac{P_s\sigma_h^2}{i\bar{I}_R}-\frac{P_s\sigma_h^2}{i\bar{I}_{P_R}}\right)^{-L_R}\left(1-\frac{P_s\sigma_h^2}{i\bar{I}_{P_R}}\right)^{-1} \tag{37d}$$

$$\lambda_5 = \left(\frac{P_s\sigma_h^2}{i\bar{I}_R}-1\right)^{-L_R}\left(\frac{P_s\sigma_h^2}{i\bar{I}_{P_R}}-1\right)^{-1} \tag{37e}$$

It is worth mentioning that in the previously derived formulas for the average error probability and ergodic capacity, the parts in the final equations that include $I_{P_{b1}}$, $I_{P_{b2}}$, $I_{C_{erg1}}$ and $I_{C_{erg2}}$ mainly affect the system performance in the case of $\frac{I_{\max}}{W} < P_t$, where W is the channel gain between the primary transmitter and the secondary receiver, and P_t is the maximum transmission power constraint of the primary transmitter node. Moreover, in the above scenario, the CR network performance does not depend on the secondary transmit power, and therefore a performance saturation phenomenon is expected. However, the secondary network can be considered as a self-controlled system performance only when $\frac{I_{\max}}{W} \geq P_t$.

V. Numerical Results and Discussions

To verify the theoretical derived expressions, extend numerical and simulation results are presented in this section. In particular, we consider a three-hop underlay CR network in our calculation. The following network parameters are considered in this section unless otherwise stated. The channel variances have been calculated based on the two-dimensional network topology, where the secondary source is located at the origin $(0, 0)$, the destination node is located at $(1, 0)$, and the primary receiver node is located at $(1, 1)$. In addition, we assume the first and second relay nodes are located at $(0.25, 0)$ and $(0.6, 0)$ respectively. The path-loss exponent is assumed to be 4. The SNR threshold is assumed to be 1 dB. Furthermore, we use these notations: $\bar{I}_{P_1}$, $\bar{I}_{P_2}$, and $\bar{I}_{P_3}$ represent the average interference powers from the primary source to the secondary receiver nodes, where the subscripts 1, 2, and 3 refer to the first relay node, the second relay and destination nodes. $\bar{I}_{R_1}$, $\bar{I}_{R_2}$, and $\bar{I}_{R_3}$ represent the average CCI powers at the corresponding receiver nodes in the three hop secondary network respectively. J is the number of antennas at the primary receiver. N_1, N_2, and N_3 are the number of receiver antennas at the relay and destination nodes respectively. L_1, L_2, and L_3 are the number of CCI signals at the relay and destination nodes respectively.

First, we start by showing the impact of multi-hop cooperative communication on the performance of the secondary network. Fig. 3 shows the outage probability vs the transmission SNR. In this figure, we compare the outage probability performance for one, two, and three hops. To make this comparison fair, only in Fig. 3, the same network parameters

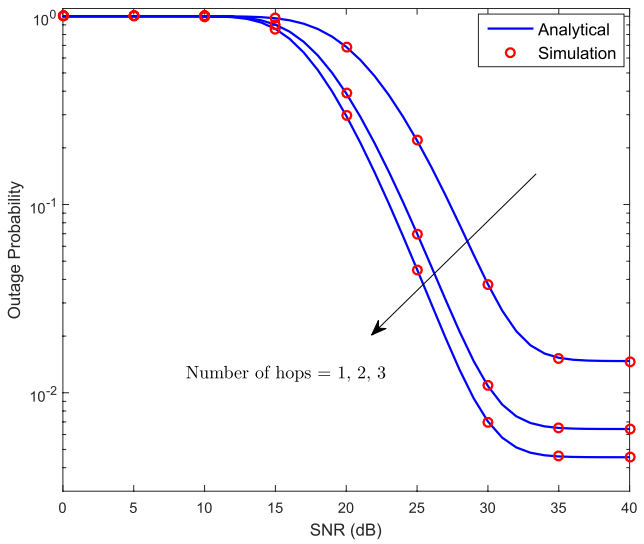

Fig. 3. Outage performance considering different number of hops in the UCRN.

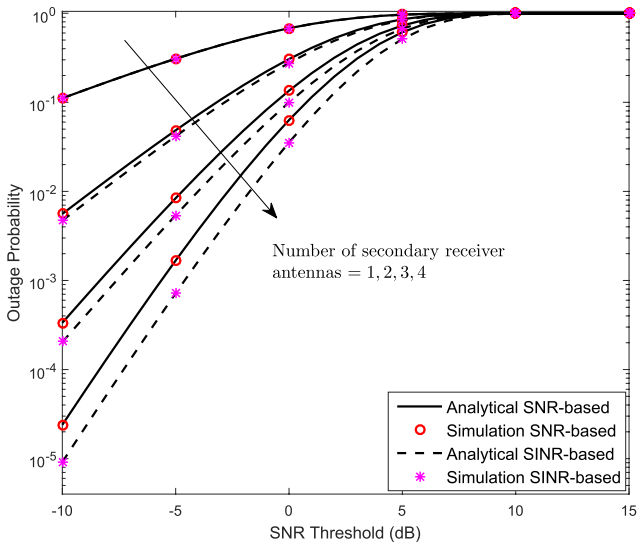

Fig. 4. Outage probability for a different number of secondary receiver antennas.

are assumed for all possible hops. For example, for the two hops network scenario, it is assumed that the relay node is located at $(1/2, 0)$, and for the three hops network scenario, the first and second relay nodes are located at $(1/3, 0)$, and $(2/3, 0)$ respectively. The parameter values for this case are as follows: $\bar{I}_P = 4$ dB, $\bar{I}_R = 2$ dB, $I_{\max} = 20$ dB, $J = 3$, $N = 2$, and $L = 4$. From these results, we can see that, for example, if the required outage performance target is 10^{-2}, then it is possible to achieve this target with two hops using the same transmission power budget. However, it is not possible to achieve this target with a direct transmission, i.e. single hop. This will prove the effectiveness of a multi-hop cooperative transmission in improving the performance of the UCRN by combating the effect of the interference power constraint. Moreover, it can be noticed that the significance of the performance improvement reduces when the number of hops increases, which is due to the fact that we have employed a DF relay protocol that means the end-to-end performance is affected by the unsuccessfully decoding at any of the relay nodes.

Fig. 4 demonstrates the outage performance vs SNR threshold for different numbers of secondary receiver antennas. The parameter values for this case are as follows: the transmit power at each of the secondary transmitters is 20 dB. In addition, $\bar{I}_{R_1}$, $\bar{I}_{R_2}$, and $\bar{I}_{R_3}$ are 2, 3, and 5 dB respectively, $\bar{I}_{P_1}$, $\bar{I}_{P_2}$, and $\bar{I}_{P_3}$ are 6, 4, and 5 dB respectively. Furthermore, $I_{\max} = 20$ dB, $J = 2$, and L_1, L_2, and L_3 are 4, 4, and 3 respectively. As expected, when the number of antennas at the SU receivers is increased, the system performance is apparently enhanced. Moreover, for the purpose of comparison, we have also plotted the outage performance for the scenario of SINR-based antenna selection using the formula in (42). An improvement in the outage performance can be observed when SINR-based antenna selection is considered. However, this consideration requires more complicated system design. Furthermore, for the case of single antenna at the secondary receiver nodes, both scenarios give the same result which partially proves the correctness and accuracy of our analysis.

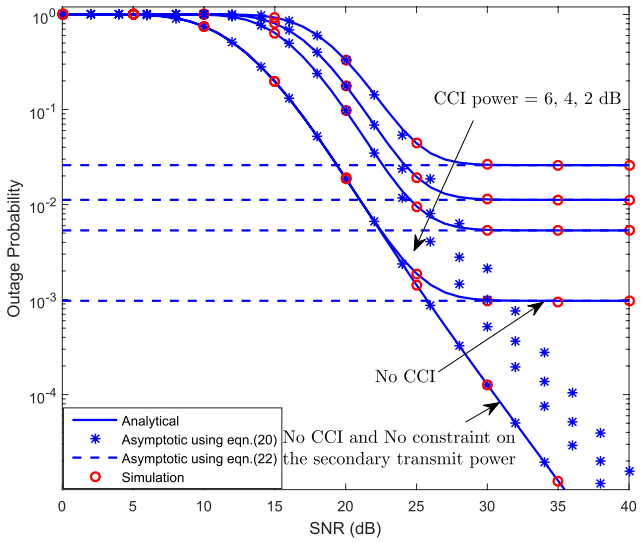

Fig. 5. Outage probability for different values of the CCI powers.

To illustrate the impact of the CCI on the CR network, Fig. 5 has been plotted, which is the outage probability performance for different CCI powers at the secondary receiver nodes. The parameter values for this case are as follows: $\bar{I}_{P_1}$, $\bar{I}_{P_2}$, and $\bar{I}_{P_3}$ are 3, 3, and 5 dB respectively. Furthermore, $I_{\max} = 15$ dB, $J = 3$, and N_1, N_2, and N_3 are 2, 3, and 4 respectively, and L_1, L_2, and L_3 are 2, 4, and 3 respectively. From these results, it can be clearly seen how the CCI power affects the performance of the secondary network, for example, when the power of the CCI signals is 6 dB, the outage performance cannot reach better than 2.59×10^{-2}, whereas when it is 2 dB, the outage performance saturates at 5.3×10^{-3}. In addition, we have plotted the approximate outage performance using derived approximate CDF expressions. It can be observed that these asymptotic expressions give relatively accurate results depending on the approximation consideration. For example, in an $I_{\max}$ dominant system, the derived expression in (22)

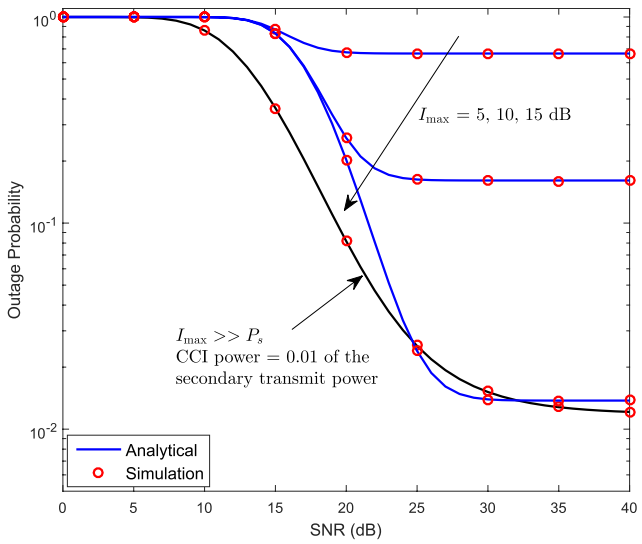

Fig. 6. Outage probability for different values of $I_{\max}$.

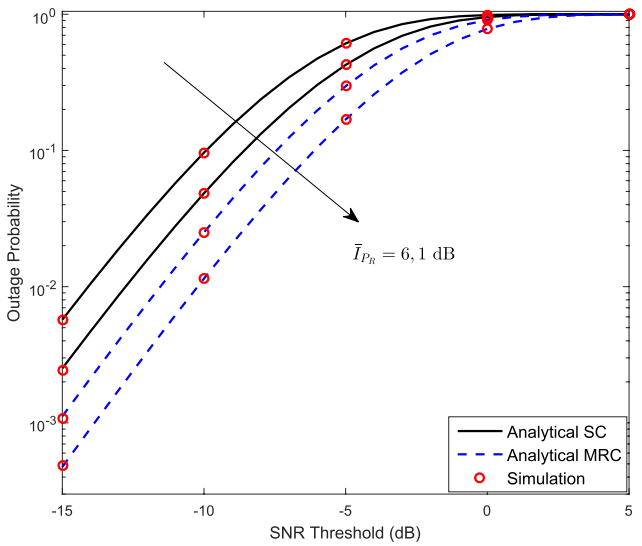

Fig. 7. Outage probability vs SNR threshold for different values of $\bar{I}_{P_R}$ and signal combining techniques at the secondary receiver nodes.

gives better results, and for a high $I_{\max}$ system, the derived expression in (20) gives more accurate results. Moreover, to compare our results with the previous work in this field, we have plotted the outage probability for the cases *a)* absence of CCI, as in [15], and *b)* absence of CCI and no constraint on the secondary transmit power, as in [13].

Fig. 6 shows the outage performance for different values of $I_{\max}$. The considered parameters are similar to the previous case, except $\bar{I}_{R_1}$, $\bar{I}_{R_2}$, and $\bar{I}_{R_3}$ are 4, 3, and 5 dB respectively. As expected, in the scenario where $I_{\max}$ is less than the transmission power of the secondary network (i.e. the $I_{\max}$ dominant region), there is an outage floor, which implies that the system performance could not improve even when the transmission power is increased. Furthermore, to better show the impact of $I_{\max}$ and a linear increase of the CCI on the performance of the UCRN, we have plotted the outage performance for the case where $I_{\max} \gg P_s$, (i.e. no restriction on the UCRN transmit nodes due to the primary receiver), and a proportional increasing of the CCI power, by 1%, is considered with regards the secondary transmission powers. It can be observed that even with no interference power constraint present, there is an outage floor. This is caused by the proportional consideration of the CCI power. From this, we deduce the severe impact of the co-channel interference power when it increases in proportion to the SU transmission power. Moreover, the plot of the result result for the case when $I_{\max} = 15$ dB, with a fixed value of CCI, outperforms the result for the linear increase of CCI consideration in a particular region. This is due to two factors: *a)* the strength of the CCI power, and *b)* the fact that the outage floor did not occur at that region for the scenario of the linear increase of the CCI power. However, the situation is reversed when the outage floor occurs.

To illustrate the effect of primary transmitter interference on the performance behaviour of the UCRN, Fig. 7 has been plotted, which shows the outage performance vs SNR threshold for different $\bar{I}_{P_R}$ and different signal combination techniques, at the secondary receiver nodes. The parameter values for this case are as follows: the secondary transmitters power and $I_{\max}$ are assumed to be 10 dB. $\bar{I}_{R_1}$, $\bar{I}_{R_2}$, and $\bar{I}_{R_3}$ are 4, 3, and 5 dB respectively. In addition, $J = 3$, the number of antennas at each of the secondary receiver nodes is 3, and $L_1 = L_2 = L_3 = 2$. Similar to the case of different CCI consideration in Fig. 5, when the considered interference power from the primary network increases, the performance of the CR network degrades. Furthermore, the MRC consideration has a significant improvement in comparison to the SC technique. However, both techniques give similar diversity gain advantage. Furthermore, in terms of the simplicity, the SC technique outperforms the MRC technique [24, p. 404]. In the previous figures and results, we have illustrated that these three factors, (i.e. $I_{\max}$, CCI, and primary transmitter interference), could severely degrade the performance of the underlay cognitive radio network depending on their consideration in the system model. More precisely, $I_{\max}$ is mainly limiting the secondary transmission power range, and CCI signals and primary transmitter interferences are deteriorating the performance of the secondary network according to their energy values. Besides, when $I_{\max}$ limits the secondary transmission power and CCI and primary transmitter interferences impact on the network performance at the same time, the probability of outage saturation occurs much faster as it can be seen in Fig. 6.

Fig. 8 shows the ABEP performance for different number of CCI signals at the SU relays and destination nodes. The parameter values for this case are as follows: $I_{\max} = 20$ dB, $\bar{I}_{R_1} = 2$ dB, $\bar{I}_{R_2} = 4$ dB, $\bar{I}_{R_3} = 3$ dB, and $\bar{I}_{P_1} = 4$ dB, $\bar{I}_{P_2} = 6$ dB, $\bar{I}_{P_3} = 5$ dB. The number of antennas at each receiver node in the system is 2. From these results, it can be seen that considering a higher number of CCI links can apparently degrade the system performance. For example, when the number of CCI signals is 5, the performance saturation occurs at 1.14×10^{-2}, while it happens at 3.0×10^{-3} when $L = 1$.

To demonstrate the impact of the number of antennas at each of the secondary receiver nodes on the ABEP performance,

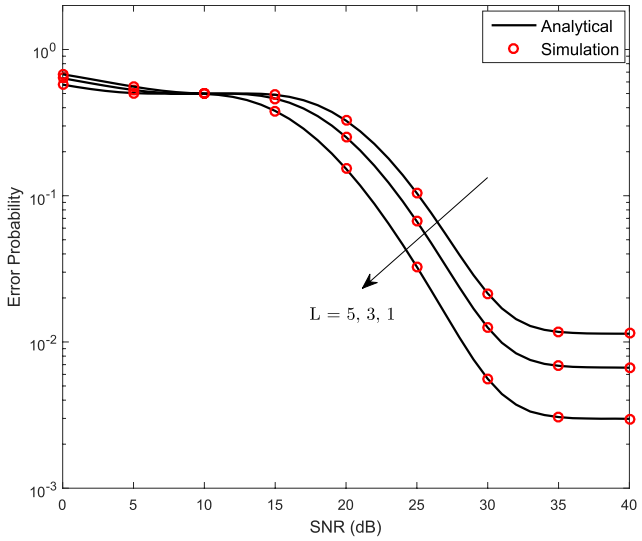

Fig. 8. Average bit error probability for a different number of CCI signals at the SU receiver nodes.

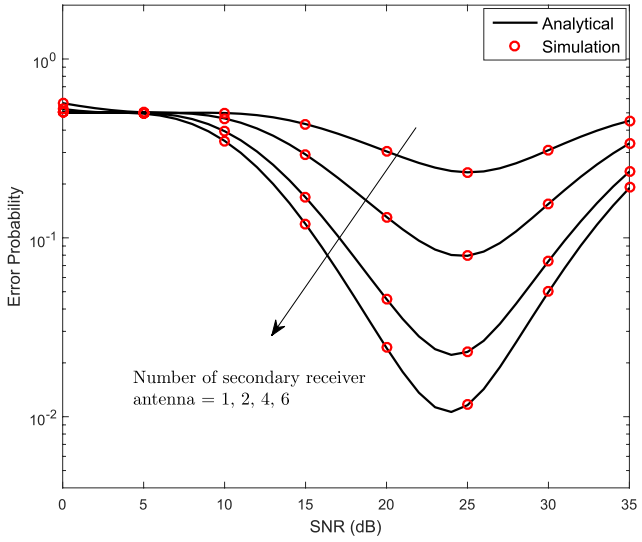

Fig. 9. Average bit error probability for a different number of antennas at the CR receiver nodes.

we have plotted Fig. 9. The parameter values for this case are as follows: the co-channel interference power is considered as increasing linearly with respect to the secondary transmission powers by 1%, (i.e. $0.01 \times P_t$, where P_t is the transmission power at each of the secondary transmit nodes). The other parameters are assumed as follows: $I_{\max} = 15$ dB, $\bar{I}_{P_1} = \bar{I}_{P_2} = 3$ dB, $\bar{I}_{P_3} = 5$ dB. $J = 3$, L_1, L_2, L_3 are 2, 1, and 3 respectively. In the above results, a performance degradation can be observed, which is mainly due to consideration of a linear increase of the CCI power and $I_{\max}$. In this case, the system performance starts degrading after $I_{\max}$ limits the secondary transmission power. In fact, this is the worst-case scenario of a secondary network performance. However, as expected, employing more antennas at the secondary receiver will enhance the error probability performance. It is worth noting that, despite the impact of interference and $I_{\max}$, the multi-antenna scheme does not lose its importance in enhancing

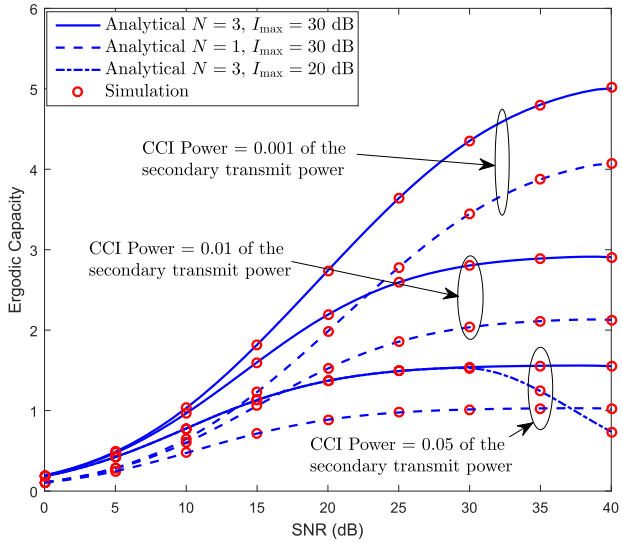

Fig. 10. Capacity performance for different values of the CCI powers and a different number of antennas at the SU receiver nodes.

the error probability performance of the UCRN. The impact of performance saturation due to the proportional increase of the interferences can be reduced by employing a multi-hop network. For example, when the interference power is studied as a proportional increase with regards to the secondary transmission powers, it is more likely that the performance saturation will occur according to the considered ratio of the interference power with the secondary transmission powers. In a multi-hop network, the source nodes can broadcast their signals at a lower power to achieve a specific performance in comparison with a direct transmission. Therefore, when the transmission power at the source nodes is reduced, the considered interference power is reduced too. Thus, improved performance will be expected.

In Fig. 10, the throughput performance has been illustrated for a different number of antennas at the secondary receiver nodes and different CCI powers. The values of the CCI powers are assumed to be increasing linearly as regards the transmission powers in the secondary nodes. The parameter values for this case are as follows: $\bar{I}_{P_1} = 6$ dB, $\bar{I}_{P_2} = 4$ dB, $\bar{I}_{P_3} = 2$ dB. $J = 2$, $L_1 = 4$, $L_2 = 3$, and $L_3 = 2$. From these results, it can be observed that the capacity saturation has occurred at 1.025 bits/sec/Hz, when the relatively higher CCI is considered, (i.e. 0.05) with a single antenna at the secondary receiver nodes. In addition, when three antennas are employed, the capacity saturation is occurred at 1.55 bits/sec/Hz. The capacity saturation in these scenarios are mainly due to the CCI power. Moreover, we have plotted the case where $I_{\max} = 20$ dB and CCI power is 5% of the secondary transmit powers. In this case, the capacity degradation is observed instead of the capacity saturation. Moreover, it can be noticed that a higher number of receiver antennas, in conjunction with the selection combining, can enhance the capacity performance of the CR network. Furthermore, it can be deduced that in an underlay CR paradigm, despite the impact of $I_{\max}$, other factors might limit the advantage of employing

a multi-antenna scheme on the network performance, such as presence of co-channel interference signals and the primary network interference. It has also been illustrated that according to their power strength consideration, they could severely degrade the CR network's performance.

Finally, from the previous results and analysis, the following observations can be summarized:

- SINR-based antenna selection gives better performance in comparison to SNR-based antenna selection. However, this approach requires more complicated configuration and is practically more challenging.
- It has been shown that the MRC technique outperforms the SC technique, however, the later one is easier to be realized in practice.
- Communication through a multi-hop relay network has the advantage of combating the impact of interference power constraint on the secondary network. In addition, it has the advantage of extending the coverage of the network.
- Performance saturation, (i.e. floor), in the system performance of the secondary network could occur due to three factors: interference from primary network, CCI power and $I_{\max}$.
- The performance saturation phenomenon could be more noticeable when the interference power is linearly increasing with the secondary transmission powers. It might cause performance reduction instead of a floor when both $I_{\max}$ and CCI have an impact on the CR network.
- An improvement in the system performance can be observed when multi-antenna receivers are considered and the best antenna selection technique is applied.
- Using multi-antenna receivers might not be an optimal solution for enhancing the system performance in power limited communication networks with the presence of interference. For example, the advantage of multi-antenna receivers, through increasing the diversity gain, can obviously be seen when there is no performance saturation. On the other hand, when performance saturation occurs, the diversity gain reduces to zero.

VI. Conclusion

In this paper, a detailed performance investigation of an uplink multi-hop multi-antenna regenerative UCRN has been presented. A more practical case scenario was assumed through the consideration of CCI in addition to the primary transmitter interference on the secondary network. Different signal combining techniques were investigated and discussed at the secondary receiver nodes. Outage probability, average error probability, and the ergodic capacity were thoroughly studied. It was shown that employing a relaying cooperative network has the advantage of enhancing the system performance through reducing the impact of the interference power constraint. Furthermore, the system performance including the impact of CCI, primary transmitter interference and interference power constraint was enhanced with a multi-antenna scheme. However, it may not provide the optimum advantage due to the constraint on the transmission power and the presence of interferences, especially when the performance saturation occurs. The impact of performance saturation can be reduced by employing a multi-hop relay network. Moreover, the severity of interference leads to performance reduction rather than performance floor, especially when its power is considered as linearly increasing with the secondary transmission power and at a relatively high ratio. Finally, different numerical and simulation examples have been presented to illustrate the performance behaviour and to support the correctness of our derived results. The analysis in this paper is significant for better understanding the characteristics and behaviour of a more practical scenario of an underlay CR network.

Appendix A
Per-Hop CDF Derivation

After substituting the formulas of $F_M\left(\frac{\gamma W}{I_{\max}}\right)$ and $f_W(w)$ into (16), we get

$$I_1 = \int_{\frac{I_{\max}}{P_s}}^{\infty} \left[1 - \sum_{i=1}^{N} \binom{N}{i} (-1)^{i+1} \frac{e^{-\frac{i\gamma w}{I_{\max}\sigma_h^2}} \sigma_h^2}{\left(\sigma_h^2 + \frac{wi\gamma \bar{I}_{P_R}}{I_{\max}}\right)} \times \left(\frac{\sigma_h^2}{\sigma_h^2 + \frac{wi\gamma \bar{I}_R}{I_{\max}}}\right)^{L_R}\right] \sum_{j=1}^{J} \binom{J}{j} (-1)^{j+1} \frac{j e^{-\frac{wj}{\sigma_{f_{sp}}^2}}}{\sigma_{f_{sp}}^2} dw. \tag{38}$$

Depending on the values of $\bar{I}_R$ and $\bar{I}_{P_R}$, there are two possible cases for the solution of the above integral. In the sections below, we derive each case in detail.

A. Case I, $\bar{I}_{P_R} = \bar{I}_R$

For this case, we change the variable in the integral so that $w = t\left(\frac{I_{\max}\sigma_{f_{sp}}^2\sigma_h^2}{jI_{\max}\sigma_h^2 + i\gamma\sigma_{f_{sp}}^2}\right) - \frac{I_{\max}\sigma_h^2}{i\gamma\bar{I}_R}$. Then, after some mathematical manipulation and with the help of [25, eq. (8.19.2)], we obtain a desired representation for the above formula.

$$I_1^I = \sum_{j=1}^{J} \binom{J}{j} (-1)^{j+1} e^{\frac{-jI_{\max}}{P_s\sigma_{f_{sp}}^2}} - \sum_{j=1}^{J}\sum_{i=1}^{N} \binom{J}{j}\binom{N}{i} (-1)^{j+i} \times \left(\frac{jI_{\max}\sigma_h^2}{i\gamma\bar{I}_R\sigma_{f_{sp}}^2}\right) e^{\left(\frac{jI_{\max}\sigma_h^2 + i\gamma\sigma_{f_{sp}}^2}{i\gamma\bar{I}_R\sigma_{f_{sp}}^2}\right)} \left(\frac{P_s\sigma_h^2}{P_s\sigma_h^2 + i\gamma\bar{I}_R}\right)^{L_R} \times E_{L_R+1}\left(\frac{\left(jI_{\max}\sigma_h^2 + i\gamma\sigma_{f_{sp}}^2\right)}{\sigma_{f_{sp}}^2\sigma_h^2} \frac{\left(P_s\sigma_h^2 + i\gamma\bar{I}_R\right)}{i\gamma\bar{I}_R P_s}\right), \tag{39}$$

where I_1^I represents the integral of I_1 for the case when $\bar{I}_{P_R} = \bar{I}_R$, and $E_n(x)$ is the exponential integral function.

B. Case II, $\bar{I}_{P_R} \neq \bar{I}_R$

For the case when $\bar{I}_{P_R} \neq \bar{I}_R$, we use the partial fraction decomposition method to solve the integral in (38) as follows

$$I_1^{II} = \sum_{j=1}^{J} \binom{J}{j} (-1)^{j+1} e^{\frac{-I_{\max} j}{P_s \sigma_{fsp}^2}} - \sum_{j=1}^{J} \sum_{i=1}^{N} \binom{J}{j} \binom{N}{i} (-1)^{j+i} \times \left(\frac{j I_{\max} \sigma_h^2}{i \sigma_{fsp}^2 \gamma \bar{I}_{P_R}} \right) \left(\frac{I_{\max} \sigma_h^2}{i \gamma \bar{I}_R} \right)^{L_R} \times \Bigg[\zeta \overbrace{\int_{\frac{I_{\max}}{P_s}}^{\infty} \frac{e^{-w\left(\frac{j I_{\max} \sigma_h^2 + i\gamma \sigma_{fsp}^2}{I_{\max} \sigma_{fsp}^2 \sigma_h^2} \right)}}{\left(\frac{I_{\max} \sigma_h^2}{i \gamma \bar{I}_{P_R}} + w \right)} dw}^{I_{21}} + \sum_{n=1}^{L_R} \times \left(\frac{i\gamma}{I_{\max} \sigma_h^2} \right)^{L_R+1-n} \Omega_n \overbrace{\int_{\frac{I_{\max}}{P_s}}^{\infty} \frac{e^{-w\left(\frac{j I_{\max} \sigma_h^2 + i\gamma \sigma_{fsp}^2}{I_{\max} \sigma_{fsp}^2 \sigma_h^2} \right)}}{\left(\frac{I_{\max} \sigma_h^2}{i \gamma \bar{I}_R} + w \right)^n} dw}^{I_{22}} \Bigg], \tag{40}$$

where $\zeta = \left(\frac{I_{\max} \sigma_h^2}{i \gamma \bar{I}_R} - \frac{I_{\max} \sigma_h^2}{i \gamma \bar{I}_{P_R}} \right)^{-L_R}$, and Ω_n is obtained by the formula given in (9). It can be observed that the above integrals (i.e. I_{21} and I_{22}), are quite similar to the previous derived integral in the first case, i.e. I_1^I in (39), therefore we write the final formula as in (41), as shown at the bottom of this page.

APPENDIX B
PER-HOP CDF USING SINR-BASED SELECTION COMBINING

In this Appendix, we represent the per-hop CDF in the case where SINR-based antenna selection is considered. The CDF can be expressed as in (42), and (43), as shown at the bottom of this page. In addition, Ω_m, and Ω_n are obtained by using (44), and (45) respectively.

$$\Omega_m = \frac{1}{(i-m)!} \frac{\partial^{i-m}}{\partial w^{i-m}} \left(\frac{1}{\bar{I}_R} + w \right)^{-iL_R} \Bigg|_{w=-\left(\frac{1}{\bar{I}_{P_R}}\right)}. \tag{44}$$

$$\Omega_n = \frac{1}{(iL_R-n)!} \frac{\partial^{iL_R-n}}{\partial w^{iL_R-n}} \left(\frac{1}{\bar{I}_{P_R}} + w \right)^{-i} \Bigg|_{w=-\left(\frac{1}{\bar{I}_R}\right)}. \tag{45}$$

Finally, it is worth mentioning that the SINR-based antenna selection technique outperforms the SNR-based antenna selection technique in terms of the performance enhancement, especially for the relatively large number of antennas at the receiver nodes. This can be seen in Fig. 4 in the numerical results section. However, the practical aspects of the SINR-based scheme are more complex to implement. Therefore, for a specific network with particular requirements, an appropriate antenna selection technique can be chosen according to the desired performance and complexity of the network.

APPENDIX C
PER-HOP CDF DERIVATION, MAXIMUM RATIO COMBINING TECHNIQUE

After substituting $F_M\left(\frac{\gamma w}{I_{\max}}\right)$ from (19) and $f_W(w)$ from (6a) into the first part integral i.e.

$$I_1^{II} = \sum_{j=1}^{J} \binom{J}{j} (-1)^{j+1} e^{-\frac{I_{\max} j}{P_s \sigma_{fsp}^2}} - \sum_{j=1}^{J} \sum_{i=1}^{N} \binom{J}{j} \binom{N}{i} (-1)^{j+i} \frac{j}{\sigma_{fsp}^2} \left(\frac{I_{\max} \sigma_h^2}{i\gamma} \right)^{L_R+1} \left(\frac{1}{\bar{I}_{P_R}} \right) \left(\frac{1}{\bar{I}_R} \right)^{L_R} \times \Bigg[\zeta \; e^{\left(\frac{j I_{\max} \sigma_h^2 + i\gamma \sigma_{fsp}^2}{i\gamma \bar{I}_{P_R} \sigma_{fsp}^2} \right)} E_1 \left(\left(\frac{j I_{\max} \sigma_h^2 + i\gamma \sigma_{fsp}^2}{\sigma_{fsp}^2 \sigma_h^2} \right) \left(\frac{P_s \sigma_h^2 + i\gamma \bar{I}_{P_R}}{i\gamma \bar{I}_{P_R} P_s} \right) \right) + \sum_{n=1}^{L_R} \Omega_n e^{\frac{j I_{\max} \sigma_h^2 + i\gamma \sigma_{fsp}^2}{i\gamma \bar{I}_R \sigma_{fsp}^2}} \left(\frac{i\gamma \bar{I}_R P_s}{P_s I_{\max} \sigma_h^2 + i\gamma \bar{I}_R I_{\max}} \right)^{n-1} E_n \left(\left(\frac{j I_{\max} \sigma_h^2 + i\gamma \sigma_{fsp}^2}{\sigma_{fsp}^2 \sigma_h^2} \right) \left(\frac{P_s \sigma_h^2 + i\gamma \bar{I}_R}{i\gamma \bar{I}_R P_s} \right) \right) \Bigg] \tag{41}$$

$$F_{\gamma_{\text{eq}}^{\text{i}}}(\gamma) = 1 + \sum_{i=1}^{N} \binom{N}{i} (-1)^i \Bigg[e^{-\frac{i\gamma}{P_s \sigma_h^2}} \left(\frac{P_s \sigma_h^2}{P_s \sigma_h^2 + \gamma \bar{I}_{P_R}} \right)^i \left(\frac{P_s \sigma_h^2}{P_s \sigma_h^2 + \gamma \bar{I}_R} \right)^{iL_R} \left(1 - e^{-\frac{I_{\max}}{P_s \sigma_{fsp}^2}} \right)^J - \sum_{j=1}^{J} \binom{J}{j} (-1)^j \frac{j I_{\max}}{\sigma_{fsp}^2} \left(\frac{1}{\bar{I}_{P_R}} \right)^i \left(\frac{1}{\bar{I}_R} \right)^{iL_R} \times \Psi_3 \Bigg] \tag{42}$$

$$\Psi_3 = \begin{cases} e^{\frac{j I_{\max} \sigma_h^2 + i\gamma \sigma_{fsp}^2}{\gamma \bar{I}_R \sigma_{fsp}^2}} \left(\frac{P_s \sigma_h^2 + \gamma \bar{I}_R}{\gamma \bar{I}_R P_s} \right) \left(\frac{\bar{I}_R P_s \sigma_h^2}{P_s \sigma_h^2 + \gamma \bar{I}_R} \right)^{iL_R+i} E_{iL_R+i} \left(\left(\frac{j I_{\max} \sigma_h^2 + i\gamma \sigma_{fsp}^2}{\sigma_{fsp}^2 \sigma_h^2} \right) \left(\frac{P_s \sigma_h^2 + \gamma \bar{I}_R}{\gamma \bar{I}_R P_s} \right) \right), & \text{if } \bar{I}_{P_R} = \bar{I}_R \\ \sum_{m=1}^{i} \Omega_m e^{\frac{j I_{\max} \sigma_h^2 + i\gamma \sigma_{fsp}^2}{\gamma \bar{I}_{P_R} \sigma_{fsp}^2}} \left(\frac{P_s \sigma_h^2 + \gamma \bar{I}_{P_R}}{\gamma \bar{I}_{P_R} P_s} \right) \left(\frac{\bar{I}_{P_R} P_s \sigma_h^2}{P_s \sigma_h^2 + \gamma \bar{I}_{P_R}} \right)^m E_m \left(\left(\frac{j I_{\max} \sigma_h^2 + i\gamma \sigma_{fsp}^2}{\sigma_{fsp}^2 \sigma_h^2} \right) \left(\frac{P_s \sigma_h^2 + \gamma \bar{I}_{P_R}}{\gamma \bar{I}_{P_R} P_s} \right) \right) \\ + \sum_{n=1}^{iL_R} \Omega_n e^{\frac{j I_{\max} \sigma_h^2 + i\gamma \sigma_{fsp}^2}{\gamma \bar{I}_R \sigma_{fsp}^2}} \left(\frac{P_s \sigma_h^2 + \gamma \bar{I}_R}{\gamma \bar{I}_R P_s} \right) \left(\frac{\bar{I}_R P_s \sigma_h^2}{P_s \sigma_h^2 + \gamma \bar{I}_R} \right)^n E_n \left(\left(\frac{j I_{\max} \sigma_h^2 + i\gamma \sigma_{fsp}^2}{\sigma_{fsp}^2 \sigma_h^2} \right) \left(\frac{P_s \sigma_h^2 + \gamma \bar{I}_R}{\gamma \bar{I}_R P_s} \right) \right), & \text{otherwise.} \end{cases} \tag{43}$$

$I_1 = \int_{\frac{I_{\max}}{P_s}}^{\infty} F_M\left(\frac{\gamma w}{I_{\max}}\right) f_W(w)\, dw$, and doing some mathematical arrangements, we get

$$\begin{aligned} I_1 = & \sum_{j=1}^{J} \binom{J}{j} (-1)^{j+1} e^{-\frac{j I_{\max}}{P_s \sigma_{f_{sp}}^2}} \\ & - \sum_{n=0}^{N-1} \sum_{i=0}^{n} \sum_{j=1}^{J} \binom{n}{i} \binom{J}{j} \frac{(-1)^{j+1}}{n!} \frac{j}{\sigma_{f_{sp}}^2 \bar{I}_{P_R}} \left(\frac{\bar{I}_{P_R}}{\bar{I}_{P_R} - \bar{I}_R}\right)^{L_R} \\ & \times \frac{1}{\left(\sigma_h^2\right)^n} \Bigg[\Gamma(i+1) \left(\frac{\gamma}{I_{\max}}\right)^{n-i-1} \left(\sigma_h^2\right)^{i+1} \\ & \times \overbrace{\int_{\frac{I_{\max}}{P_s}}^{\infty} \frac{(w)^n\, e^{-w\left(\frac{j}{\sigma_{f_{sp}}^2} + \frac{\gamma}{I_{\max}\sigma_h^2}\right)}}{\left(\frac{I_{\max}\sigma_h^2}{\gamma \bar{I}_{P_R}} + w\right)^{i+1}} dw}^{I_1^a} \\ & - \sum_{m=0}^{L_R-1} \frac{(m+i)! \left(\sigma_h^2\right)^n}{m!} \left(\frac{\bar{I}_{P_R} - \bar{I}_R}{\bar{I}_{P_R} \bar{I}_R}\right)^m \\ & \times \left(\frac{\gamma}{I_{\max}\sigma_h^2}\right)^{n-m-i-1} \\ & \times \overbrace{\int_{\frac{I_{\max}}{P_s}}^{\infty} \frac{(w)^n\, e^{-w\left(\frac{j}{\sigma_{f_{sp}}^2} + \frac{\gamma}{I_{\max}\sigma_h^2}\right)}}{\left(\frac{I_{\max}\sigma_h^2}{\gamma \bar{I}_R} + w\right)^{m+i+1}} dw}^{I_1^b} \Bigg]. \end{aligned} \tag{46}$$

For the purpose of simplicity and mathematical tractability, we use these entities to define the following terms; $\hat{\beta}_1 = \frac{\gamma}{I_{\max}\sigma_h^2}$, $\hat{\beta}_2 = \frac{I_{\max}\sigma_h^2}{\gamma \bar{I}_{P_R}}$, $\hat{\beta}_3 = \frac{I_{\max}\sigma_h^2}{\gamma \bar{I}_R}$, and $\hat{\beta}_4 = \frac{j}{\sigma_{f_{sp}}^2}$. Then, we exchange the variable in the I_1^b integral formula, so that $w = \frac{x}{\hat{\beta}_1 + \hat{\beta}_4} - \hat{\beta}_2$. Subsequently, we use the Binomial expansion to further simplify the integral formula, and after some mathematical manipulation we obtain

$$\begin{aligned} I_1^a = & \sum_{n_1=0}^{n} \binom{n}{n_1} (-\hat{\beta}_2)^{n-n_1} \left(\hat{\beta}_1 + \hat{\beta}_4\right)^{i-n_1} e^{\hat{\beta}_2\left(\hat{\beta}_1 + \hat{\beta}_4\right)} \\ & \times \int_{\left(\frac{I_{\max}}{P_s} + \hat{\beta}_2\right)\left(\hat{\beta}_1 + \hat{\beta}_4\right)}^{\infty} \frac{e^{-x}}{x^{i+1-n_1}}\, dx. \end{aligned} \tag{47}$$

Finally, with the help of [25, eq. (8.19.2)], we arrive at the desired representation for the above formula. Similar steps can be repeated to solve the integral formula I_1^b. Therefore, by combining the above derived expressions, we are able to get an exact formula for the per hop CDF in the scenario where the MRC technique is considered at the secondary receiver nodes, and the formula can be written as in (17). The formulas of I_{mrc}^2 and I_{mrc}^1 are represented as in (48) and (49), as shown at the bottom of this page.

APPENDIX D
ERROR PROBABILITY DERIVATION

To obtain a closed-form expression for the average bit error probability, the derived CDF in (7) is used. We start by substituting (7) into (26), as a result, we get the average per-hop error probability integral expression for two cases, (i.e. $\bar{I}_{P_R} = \bar{I}_R$, and $\bar{I}_{P_R} \neq \bar{I}_R$). In derivations below, we use the following notation to make the derivation more tractable and easier to follow. First, let $\alpha_1 = \frac{P_s \sigma_h^2}{i}$, $\alpha_2 = \frac{P_s \sigma_h^2}{i \bar{I}_{P_R}}$, $\alpha_3 = \frac{P_s \sigma_h^2}{i \bar{I}_R}$, $\alpha_4 = \frac{j I_{\max} \sigma_h^2}{i \bar{I}_R \sigma_{f_{sp}}^2}$, $\alpha_5 = \frac{j I_{\max} \sigma_h^2}{i \bar{I}_{P_R} \sigma_{f_{sp}}^2}$, $\alpha_6 = \frac{j I_{\max}}{P_s \sigma_{f_{sp}}^2} + \frac{1}{\bar{I}_R}$, and $\alpha_7 = \frac{j I_{\max}}{P_s \sigma_{f_{sp}}^2} + \frac{1}{\bar{I}_{P_R}}$. Then, let

$$\Upsilon_1 = \alpha_2\, \alpha_3^{L_R} \left(1 - e^{-\frac{I_{\max}}{P_s \sigma_{f_{sp}}^2}}\right)^J, \tag{50a}$$

$$\Upsilon_2 = \frac{e^{\left(\frac{\alpha_4}{\gamma} + \frac{1}{\bar{I}_R}\right)}}{\gamma\ (\alpha_3 + \gamma)^{L_R}} E_{L_R+1}\left(\frac{\alpha_4}{\gamma} + \frac{\gamma}{\alpha_1} + \alpha_6\right), \tag{50b}$$

$$\begin{aligned} \Upsilon_3 = & \left(\frac{\bar{I}_{P_R}}{\bar{I}_{P_R} - \bar{I}_R}\right)^{L_R} \frac{e^{\left(\frac{\alpha_5}{\gamma} + \frac{1}{\bar{I}_{P_R}}\right)}}{\gamma} E_1\left(\frac{\alpha_5}{\gamma} + \frac{\gamma}{\alpha_1} + \alpha_7\right) \\ & + \sum_{n=1}^{L_R} \Omega_n \frac{\alpha_1^{n-1}}{\bar{I}_R^{L_R}} \frac{e^{\left(\frac{\alpha_4}{\gamma} + \frac{1}{\bar{I}_R}\right)}}{\gamma\ (\alpha_3 + \gamma)^{n-1}} E_n\left(\frac{\alpha_4}{\gamma} + \frac{\gamma}{\alpha_1} + \alpha_6\right). \end{aligned} \tag{50c}$$

C. First Case (i.e. $\bar{I}_{P_R} = \bar{I}_R$)

For this case, the integral formula contains three main parts. In this section, the detailed steps and explanation of each part are presented. The integral in the first part is obtained with

$$I_{mrc}^2 = \left(\frac{\gamma}{P_s \sigma_h^2}\right)^n e^{-\frac{\gamma}{P_s \sigma_h^2}} \left(1 - e^{-\frac{I_{\max}}{P_s \sigma_{f_{sp}}^2}}\right)^J \times \left[\frac{\Gamma(i+1)}{\left(\frac{1}{\bar{I}_{P_R}} + \frac{\gamma}{P_s \sigma_h^2}\right)^{i+1}} - \sum_{m=0}^{L_R-1} \frac{1}{m!} \left(\frac{\bar{I}_{P_R} - \bar{I}_R}{\bar{I}_{P_R} \bar{I}_R}\right)^m \frac{\Gamma(m+i+1)}{\left(\frac{1}{\bar{I}_R} + \frac{\gamma}{P_s \sigma_h^2}\right)^{m+i+1}}\right] \tag{48}$$

$$\begin{aligned} I_{mrc}^1 = & \sum_{j=1}^{J} \binom{J}{j} (-1)^{j+1} \left(\frac{j}{\sigma_{f_{sp}}^2}\right) \left(\sigma_h^2\right)^{i+1-n} \times \Bigg[\sum_{n_1=0}^{n} \binom{n}{n_1} (-\hat{\beta}_2)^{n-n_1} \Gamma(i+1) \left(\frac{\gamma}{I_{\max}}\right)^{n-i-1} \left(\hat{\beta}_1 + \hat{\beta}_4\right)^{i-n_1} \\ & \times e^{\hat{\beta}_2\left(\hat{\beta}_1 + \hat{\beta}_4\right)} E_{i+1-n_1}\left(\left(\frac{I_{\max}}{P_s} + \hat{\beta}_2\right)\left(\hat{\beta}_1 + \hat{\beta}_4\right)\right) - \sum_{m=0}^{L_R-1} \sum_{n_2=0}^{n} \binom{n}{n_2} (-\hat{\beta}_3)^{n-n_2} \frac{\Gamma(m+i+1)}{\Gamma(m+1)} \left(\sigma_h^2\right)^m \left(\frac{\bar{I}_{P_R} - \bar{I}_R}{\bar{I}_{P_R} \bar{I}_R}\right)^m \\ & \times \left(\frac{\gamma}{I_{\max}}\right)^{n-m-i-1} \left(\hat{\beta}_1 + \hat{\beta}_4\right)^{m+i-n_2} e^{\hat{\beta}_3\left(\hat{\beta}_1 + \hat{\beta}_4\right)} E_{m+i+1-n_2}\left(\left(\frac{I_{\max}}{P_s} + \hat{\beta}_3\right)\left(\hat{\beta}_1 + \hat{\beta}_4\right)\right) \Bigg]. \end{aligned} \tag{49}$$

the help of [25, eq. (5.2.1)]. In this derivation, some basic functions manipulation should be taken into account, such as; $n! = \Gamma(n+1)$ and $\Gamma(1/2) = \sqrt{\pi}$. We write the second part as follows

$$\bar{P}_{b_I}^{2}(e) = \Upsilon_1 \frac{a}{2}\sqrt{\frac{b}{\pi}} \int_0^{\infty} \frac{e^{-b\gamma}}{\sqrt{\gamma}} \frac{e^{-\frac{\gamma}{\alpha_1}}}{(\alpha_3+\gamma)^{L_R+1}}\, d\gamma, \tag{51}$$

For the second part i.e. $\bar{P}_{b_I}^{2}(e)$ we first exchange the variable in the integral as $\gamma = t\alpha_3$. Then, by using [25, eq. (13.4.4)] the desired formula can be obtained

$$\bar{P}_{b_I}^{2}(e) = \Upsilon_1 \frac{a}{2}\sqrt{b}\left(b+\frac{1}{\alpha_1}\right)^{L_R+\frac{1}{2}} \times \mathrm{U}\left(L_R+1, L_R+\frac{3}{2}, \left(b+\frac{1}{\alpha_1}\right)\alpha_3\right). \tag{52}$$

In (52), $U(\alpha, \beta, z)$ represents the confluent hypergeometric function. We can write the third part as

$$\bar{P}_{b_I}^{3}(e) = \frac{a}{2}\sum_{j=1}^{J}\binom{J}{j}(-1)^j \alpha_4 \alpha_3^{L_R}\sqrt{\frac{b}{\pi}} \times \int_0^{\infty} \frac{e^{-\gamma b}}{\sqrt{\gamma}} \Upsilon_2 d\gamma, \tag{53}$$

where $\bar{P}_{b_I}^{3}(e)$ is the third part of the first case ABEP equation. To the best of our knowledge, it would be quite difficult, if not impossible to solve the above integral. In addition, it should be noticed that there is more than one term that includes the exponential integral function in the CDF formula. Therefore, it is not an efficient method to approximate these terms. However, these terms can be determined numerically by utilizing different software tools, for example, Matlab, Maple and Mathematica. Therefore, we determine this part of the formula numerically and write the above formula as

$$\bar{P}_{b_I}^{3}(e) = \frac{a}{2}\sum_{j=1}^{J}\binom{J}{j}(-1)^j\ \alpha_4\ \alpha_3^{L_R}\ \sqrt{\frac{b}{\pi}} I_{P_{b1}}. \tag{54}$$

Therefore, we determine the value of $I_{P_{b1}}$ numerically using the following integral formula

$$I_{P_{b1}} = \int_0^{\infty} \frac{e^{-\gamma b}}{\sqrt{\gamma}}\ \Upsilon_2\ d\gamma, \tag{55}$$

where Υ_2 is defined in (50b).

D. Second Case (i.e. $\bar{I}_{P_R} \neq \bar{I}_R$)

For the second case, we get a formula that has three integral parts. The first part is similar to the first part of the previous case. The part two, second case of the ABEP formula, can be expressed as

$$\bar{P}_{b_{II}}^{2}(e) = \Upsilon_1 \frac{a}{2}\sqrt{\frac{b}{\pi}} \int_0^{\infty} \frac{e^{-\gamma\left(b+\frac{1}{\alpha_1}\right)}\gamma^{-\frac{1}{2}}}{(\alpha_2+\gamma)\times(\alpha_3+\gamma)^{L_R}} d\gamma, \tag{56}$$

As previously mentioned and demonstrated, using the partial fraction can make some expressions simpler. Therefore, we employ this technique to make the integral expression in (56) easier to manipulate as follows

$$\bar{P}_{b_{II}}^{2}(e) = \Upsilon_1 \frac{a}{2}\sqrt{\frac{b}{\pi}} \int_0^{\infty} e^{-\gamma\left(b+\frac{1}{\alpha_1}\right)} \times \gamma^{-\frac{1}{2}}\left[\sum_{m_1=1}^{L_R}\frac{\mu_{m_1}}{(\alpha_3+\gamma)^{m_1}} + \frac{\mu_2}{(\alpha_2+\gamma)}\right] d\gamma, \tag{57}$$

where μ_{m_1}, and μ_2 are calculated using the expressions provided in (31a, and 31b) respectively. Therefore, we rewrite each sub part for the second part as $\bar{P}_{b_{II}}^{21}(e)$, and $\bar{P}_{b_{II}}^{22}(e)$ respectively. Next, we exchange the variable for $\bar{P}_{b_{II}}^{21}(e)$ so that $\gamma = t^2\alpha_2$. Then, by comparing our formula with [25, eq. (7.7.1)], and after performing some mathematical manipulations and arrangements the desired formula can be obtained as

$$\bar{P}_{b_{II}}^{21}(e) = \Upsilon_1 \frac{a}{2}\sqrt{\frac{b\pi}{\alpha_2}}\mu_2 e^{\alpha_2\left(b+\frac{1}{\alpha_1}\right)}\mathrm{erfc}\left(\sqrt{\alpha_2\left(b+\frac{1}{\alpha_1}\right)}\right). \tag{58}$$

In (58), erfc (x) represents the complementary error function. The solution of the integral formula for $\bar{P}_{b_{II}}^{22}(e)$ is quite similar to the second part of the first case, (i.e. $\bar{P}_{b_I}^{2}(e)$). Therefore, it can be solved as

$$\bar{P}_{b_{II}}^{22}(e) = \Upsilon_1 \times\ \frac{a}{2}\sqrt{b}\sum_{m_1=1}^{L_R}\mu_{m_1}\left(b+\frac{1}{\alpha_1}\right)^{m_1-\frac{1}{2}} \times \mathrm{U}\left(m_1, m_1+\frac{1}{2}, \left(b+\frac{1}{\alpha_1}\right)\alpha_3\right). \tag{59}$$

Similar to the third part of the first case, we evaluate numerically the third part of the second case.

$$\bar{P}_{b_{II}}^{3}(e) = \frac{a}{2}\sum_{j=1}^{J}\binom{J}{j}(-1)^j\ \alpha_5\ \sqrt{\frac{b}{\pi}} I_{P_{b2}}. \tag{60}$$

The value of $I_{P_{b2}}$ in (60) is determined using the following integral formula

$$I_{P_{b2}} = \int_0^{\infty} \frac{e^{-\gamma b}}{\sqrt{\gamma}}\ \Upsilon_3\ d\gamma, \tag{61}$$

where Υ_3 is defined in (50c). Finally, a closed-form expression for the average bit error probability can be obtained through summing all derived parts and substituting the notations that we have used for the derivations, it is represented in the formula in (28).

APPENDIX E
ERGODIC CAPACITY DERIVATION

To derive a closed-form ergodic capacity formula for the multi-hop UCRN, we use the formula of the per-hop equivalent CDF. This can be obtained by substituting (7) into (32). This will give us an integral formula for the two different cases: *case I* (i.e. $\bar{I}_{PR} = \bar{I}_R$) and *case II* (i.e. $\bar{I}_{PR} \neq \bar{I}_R$). In this Appendix, the detailed steps of the derivation for both cases are presented. In addition, we use the same notation that we defined in Appendix D.

E. First Case (i.e. $\bar{I}_{P_R} = \bar{I}_R$)

For the first case, the formula has two integral parts. We represent the first part by $C^1_{erg_{\rm I}}$, and the second part by $C^2_{erg_{\rm I}}$. The first integral part has the following integral form

$$C^1_{erg_{\rm I}} = \Upsilon_1 \int_0^\infty \frac{1}{(1+\gamma)} \frac{e^{-\frac{\gamma}{\alpha_1}}}{(\alpha_3+\gamma)^{L_R+1}}\, d\gamma, \tag{62}$$

where Υ_1 is defined in (50a). With the help of partial fraction, the above integral expression can be written in a simpler form. More specifically, it can be represented by two terms as

$$C^1_{erg_{\rm I}} = \Upsilon_1 \int_0^\infty e^{\frac{-\gamma}{\alpha_1}} \left[\frac{\lambda_1}{(1+\gamma)} + \sum_{r_2=1}^{L_R+1} \frac{\lambda_{r_2}}{(\alpha_3+\gamma)^{r_2}} \right] d\gamma. \tag{63}$$

In (63), λ_1, and λ_{r_2} are determined using formulas provided in (37a), and (37b) respectively. *In the above formula, we have assumed that $P_s\sigma_h^2 \neq i\bar{I}_R$, i.e. $\alpha_3 \neq 1$. In fact, in the case of $\alpha_3 = 1$, there will be an extra possible case, which is similar to the existing forms.* Then, after some straightforward mathematical manipulation and with the help of [25, eq. (8.19.2)], we can get a desired representation for the integral formula in (62).

$$C^1_{erg_{\rm I}} = \Upsilon_1 \Bigg[\lambda_1 e^{\frac{1}{\alpha_1}} E_1\left(\frac{1}{\alpha_1}\right) + \sum_{r_2=1}^{L_R+1} \lambda_{r_2} (\alpha_3)^{1-r_2} e^{\frac{\alpha_3}{\alpha_1}} E_{r_2}\left(\frac{\alpha_3}{\alpha_1}\right) \Bigg]. \tag{64}$$

Part $C^2_{erg_{\rm I}}$ of the ergodic capacity integral formula has the following form

$$C^2_{erg_{\rm I}} = \sum_{j=1}^{J} \binom{J}{j} (-1)^j\ \alpha_4\ \alpha_3^{L_R} \int_0^\infty \frac{\Upsilon_2}{1+\gamma}\, d\gamma, \tag{65}$$

where Υ_2 is defined in (50b). We keep the integral in this part and solve it numerically. Therefore, it can be obtained as $C^2_{erg_{\rm I}} = \sum_{j=1}^{J} \binom{J}{j}(-1)^j\ \alpha_4\ \alpha_3^{L_R}\ I_{C_{erg1}}$, where

$$I_{C_{erg1}} = \int_0^\infty \frac{\Upsilon_2}{1+\gamma}\, d\gamma. \tag{66}$$

F. Second Case (i.e. $\bar{I}_{P_R} \neq \bar{I}_R$)

In this case, the integral formula has two parts. We denote part one by $C^1_{erg_{\rm II}}$, and part two by $C^2_{erg_{\rm II}}$. In this section, the derivation steps for each part are presented.

$$C^1_{erg_{\rm II}} = \Upsilon_1 \int_0^\infty \frac{e^{-\frac{\gamma}{\alpha_1}}}{(1+\gamma)(\alpha_2+\gamma)(\alpha_3+\gamma)^{L_R}}\, d\gamma. \tag{67}$$

The above integral formula is mathematically difficult to manipulate, by employing the partial fraction decomposition technique, we represent the integral in a simpler form as

$$C^1_{erg_{\rm II}} = \Upsilon_1 \int_0^\infty e^{-\frac{\gamma}{\alpha_1}} \left[\sum_{r_3=1}^{L_R} \frac{\lambda_{r_3}}{(\alpha_3+\gamma)^{r_3}} + \frac{\lambda_4}{(\alpha_2+\gamma)} + \frac{\lambda_5}{(1+\gamma)} \right] d\gamma. \tag{68}$$

In (68) λ_{r_3}, λ_4 and λ_5 are determined using formulas provided in (37c), (37d) and (37e) respectively. *In the above formula, we have assumed that $P_s\sigma_h^2 \neq i\bar{I}_{P_R}$ and/or $P_s\sigma_h^2 \neq i\bar{I}_R$. If the following scenarios are considered, there will be two extra possible cases, which are similar to the existing forms.* It can be observed that the integrals in (68) have similar forms to the integrals in the first case, i.e. $C^1_{erg_{\rm I}}$. Therefore, the final formula can be written as

$$C^1_{erg_{\rm II}} = \Upsilon_1 \Bigg[\sum_{r_3=1}^{L_R} \lambda_{r_3} (\alpha_3)^{1-r_3} e^{\frac{\alpha_3}{\alpha_1}} E_{r_3}\left(\frac{\alpha_3}{\alpha_1}\right) + \lambda_4 e^{\frac{\alpha_2}{\alpha_1}} E_1\left(\frac{\alpha_2}{\alpha_1}\right) + \lambda_5 e^{\frac{1}{\alpha_1}} E_1\left(\frac{1}{\alpha_1}\right) \Bigg]. \tag{69}$$

Part two in the second case of the ergodic capacity integral formula can be written as

$$C^2_{erg_{\rm II}} = \sum_{j=1}^{J} \binom{J}{j} (-1)^j\ \alpha_4\ \alpha_3^{L_R} \int_0^\infty \frac{\Upsilon_2}{1+\gamma}\, d\gamma, \tag{70}$$

where Υ_3 is defined in (50c). Similar to the second part of the first case, we numerically evaluate $C^2_{erg_{\rm II}}$ as $C^2_{erg_{\rm II}} = \sum_{j=1}^{J} \binom{J}{j}(-1)^j\ \alpha_5\ I_{C_{erg2}}$, where

$$I_{C_{erg2}} = \int_0^\infty \frac{\Upsilon_3}{1+\gamma}\, d\gamma. \tag{71}$$

Finally, a closed-form ergodic capacity expression for one hop of the secondary network can be obtained by summing all parts and substituting the notations that we have used for the derivations, and it can be written as in (34).

REFERENCES

[1] A. Goldsmith, S. A. Jafar, I. Maric, and S. Srinivasa, "Breaking spectrum gridlock with cognitive radios: An information theoretic perspective," *Proc. IEEE*, vol. 97, no. 5, pp. 894–914, Apr. 2009.

[2] Y.-C. Liang, Y. Zeng, E. C. Y. Peh, and A. T. Hoang, "Sensing-throughput tradeoff for cognitive radio networks," *IEEE Trans. Wireless Commun.*, vol. 7, no. 4, pp. 1326–1337, Apr. 2008.

[3] K. B. Letaief and W. Zhang, "Cooperative communications for cognitive radio networks," *Proc. IEEE*, vol. 97, no. 5, pp. 878–893, May 2009.

[4] S. S. Ikki and S. Aissa, "Effects of co-channel interference on the error probability performance of multi-hop relaying networks," in *Proc. IEEE Global Telecommun. Conf. (GLOBECOM)*, Dec. 2011, pp. 1–5.

[5] Y. Huang, F. S. Al-Qahtani, C. Zhong, Q. Wu, J. Wang, and H. M. Alnuweiri, "Cognitive MIMO relaying networks with primary user's interference and outdated channel state information," *IEEE Trans. Commun.*, vol. 62, no. 12, pp. 4241–4254, Dec. 2014.

[6] Q. Li *et al.*, "MIMO techniques in WiMAX and LTE: A feature overview," *IEEE Commun. Mag.*, vol. 48, no. 5, pp. 86–92, May 2010.

[7] M. Hanif, H. C. Yang, and M. S. Alouini, "Receive antenna selection for underlay cognitive radio with instantaneous interference constraint," *IEEE Signal Process. Lett.*, vol. 22, no. 6, pp. 738–742, Jun. 2015.

[8] Y. Zhang, C. Ji, W. Q. Malik, D. O'Brien, and D. J. Edwards, "Receive antenna selection for MIMO systems over correlated fading channels," *IEEE Trans. Wireless Commun.*, vol. 8, no. 9, pp. 4393–4399, Sep. 2009.

[9] A. F. Molisch, M. Z. Win, Y.-S. Choi, and J. H. Winters, "Capacity of MIMO systems with antenna selection," *IEEE Trans. Wireless Commun.*, vol. 4, no. 4, pp. 1759–1772, Jul. 2005.

[10] Y. Deng, M. Elkashlan, N. Yang, P. L. Yeoh, and R. K. Mallik, "Impact of primary network on secondary network with generalized selection combining," *IEEE Trans. Veh. Technol.*, vol. 64, no. 7, pp. 3280–3285, Jul. 2015.

[11] Y. Huang, J. Wang, Q. Wu, C. Zhong, and C. Li, "Outage performance of spectrum sharing systems with MRC diversity under multiple primary user's interference," *IEEE Commun. Lett.*, vol. 18, no. 4, pp. 576–579, Apr. 2014.
[12] J. Hussein, S. Ikki, S. Boussakta, and C. Tsimenidis, "Performance study of the dual-hop underlay cognitive network in the presence of co-channel interference," in *Proc. IEEE 81st Veh. Technol. Conf. (VTC Spring)*, May 2015, pp. 1–5.
[13] T. Q. Duong, V. N. Q. Bao, H. Tran, G. C. Alexandropoulos, and H.-J. Zepernick, "Effect of primary network on performance of spectrum sharing AF relaying," *Electron. Lett.*, vol. 48, no. 1, pp. 25–27, Jan. 2012.
[14] Q. Wu, Z. Zhang, and J. Wang, "Outage analysis of cognitive relay networks with relay selection under imperfect CSI environment," *IEEE Commun. Lett.*, vol. 17, no. 7, pp. 1297–1300, Jul. 2013.
[15] P. L. Yeoh, M. Elkashlan, T. Q. Duong, N. Yang, and D. B. da Costa, "Transmit antenna selection for interference management in cognitive relay networks," *IEEE Trans. Veh. Technol.*, vol. 63, no. 7, pp. 3250–3262, Sep. 2014.
[16] Y. Huang, F. Al-Qahtani, Q. Wu, C. Zhong, J. Wang, and H. Alnuweiri, "Outage analysis of spectrum sharing relay systems with multiple secondary destinations under primary user's interference," *IEEE Trans. Veh. Technol.*, vol. 63, no. 7, pp. 3456–3464, Sep. 2014.
[17] H. Huang, N. C. Beaulieu, Z. Li, and J. Si, "On the performance of underlay cognitive multisource multirelay cooperative networks," *IEEE Commun. Lett.*, vol. 19, no. 4, pp. 605–608, Apr. 2015.
[18] K. Ho-Van, P. C. Sofotasios, G. C. Alexandropoulos, and S. Freear, "Bit error rate of underlay decode-and-forward cognitive networks with best relay selection," *J. Commun. Netw.*, vol. 17, no. 2, pp. 162–171, Apr. 2015.
[19] A. Afana, V. Asghari, A. Ghrayeb, and S. Affes, "On the performance of cooperative relaying spectrum-sharing systems with collaborative distributed beamforming," *IEEE Trans. Commun.*, vol. 62, no. 3, pp. 857–871, Mar. 2014.
[20] X. Zhang, Y. Zhang, Z. Yan, J. Xing, and W. Wang, "Performance analysis of cognitive relay networks over Nakagami-*m* fading channels," *IEEE J. Sel. Areas Commun.*, vol. 33, no. 5, pp. 865–877, May 2015.
[21] V. N. Q. Bao, T. Q. Duong, and C. Tellambura, "On the performance of cognitive underlay multihop networks with imperfect channel state information," *IEEE Trans. Commun.*, vol. 61, no. 12, pp. 4864–4873, Dec. 2013.
[22] J. Hussein, S. Ikki, S. Boussakta, and C. Tsimenidis, "Performance analysis of opportunistic scheduling in dual-hop multi-user underlay cognitive network in the presence of co-channel interference," *IEEE Trans. Veh. Technol.*, to be published.
[23] S. S. Ikki, P. Ubaidulla, and S. Aissa, "Performance study and optimization of cooperative diversity networks with co-channel interference," *IEEE Trans. Wireless Commun.*, vol. 13, no. 1, pp. 14–23, Jan. 2014.
[24] M. K. Simon and M.-S. Alouini, *Digital Communication Over Fading Channels*, 2nd ed. Hoboken, NJ, USA: Wiley, 2005.
[25] F. W. J. Olver, D. W. Lozier, R. F. Boisvert, and C. W. Clark, Eds., *NIST Handbook of Mathematical Functions*. New York, NY, USA: Cambridge Univ. Press, 2010.
[26] B. A. Ogunnaike, *Random Phenomena: Fundamentals of Probability and Statistics for Engineers*. New York, NY, USA: CRC Press, 2010.

Jamal Ahmed Hussein (S'04) received the B.Sc. degree (Hons.) in electrical engineering from the Electrical Department, College of Engineering, University of Salahaddin, Erbil, Iraq, in 2001, and the M.Sc. degree in electrical engineering from the Electrical Department, College of Engineering, University of Sulaimani, Sulaimani, Iraq, in 2007. He is currently pursuing the Ph.D. degree in communication and signal processing with the School of Electrical and Electronic Engineering, Newcastle University, Newcastle Upon Tyne, U.K. His research interests include wireless communication, cooperative communication, cognitive radio, and energy harvesting.

Salama S. Ikki received the B.S. degree from Al-Isra University, Amman, Jordan, in 1996, the M.Sc. degree from The Arab Academy for Science and Technology and Maritime Transport, Alexandria, Egypt, in 2002, and the Ph.D. degree from Memorial University, St. Johns, NL, Canada, in 2009, all in electrical engineering. From 2009 to 2010, he was a Post-Doctoral Researcher with the University of Waterloo, ON, Canada. From 2010 to 2012, he was a Research Assistant with INRS, University of Quebec, Montreal, QC, Canada. He is currently an Assistant Professor of wireless communications with Lakehead University, Thunder Bay, ON, Canada. He has authored over 100 journal and conference papers and over 2000 citations and an H-index of 23. His research interests include cooperative networks, multiple-input multiple-output, spatial modulation, and wireless sensor networks. He has served as a Technical Program Committee Member for various conferences, including the IEEE International Conference on Communications, the IEEE Global Communications Conference, the IEEE Wireless Communications and Networking Conference, the IEEE Spring/Fall Vehicular Technology Conference, and the IEEE International Symposium on Personal, Indoor and Mobile Communications. He currently serves on the Editorial Board of the IEEE COMMUNICATIONS LETTERS and *IET Communications*. He received a best paper award for his paper published in the *EURASIP Journal on Advanced Signal Processing*. He also received the IEEE COMMUNICATIONS LETTERS, the IEEE WIRELESS COMMUNICATIONS LETTERS and the IEEE TRANSACTIONS ON VEHICULAR TECHNOLOGY Exemplary Reviewer certificates for 2012, 2012, and 2014, respectively.

Said Boussakta (S'89–M'90–SM'04) received the Ingenieur d'Etat degree in electronics engineering from the National Polytechnic Institute of Algiers, Algeria, in 1985, and the Ph.D. degree in electrical engineering from Newcastle University, U.K., in 1990. From 1990 to 1996, he was with Newcastle University as a Senior Research Associate in digital signal processing. From 1996 to 2000, he was with the University of Teesside, UK, as a Senior Lecturer in communication engineering. From 2000 to 2006, he was with the University of Leeds as a Reader in digital communications and signal processing. He is currently a Professor of communications and signal processing with the School of Electrical and Electronic Engineering, Newcastle University, where he is lecturing in communication networks and signal processing subjects. His research interests are in the areas of fast DSP algorithms, digital communications, communication network systems, cryptography, and digital signal/image processing. He has authored or co-authored over 200 publications and served as Chair for Signal Processing for Communications Symposium in ICC06, ICC07, ICC08, ICC2010 and ICC2013. Prof Boussakta is a Fellow of the IET, and a Senior Member of the IEEE Communications and Signal Processing Societies.

Charalampos C. Tsimenidis (M'05–SM'12) received the M.Sc. (Hons.) and the Ph.D. degree in communications and signal processing from Newcastle University in 1999 and 2002, respectively. He is currently a Senior Lecturer in signal processing for communications with the School of Electrical and Electronic Engineering, Newcastle University, U.K. His main research interests are in the area of adaptive array receivers for wireless communications including demodulation algorithms and protocol design for underwater acoustic channels. He has authored over 180 conference and journal papers, supervised successfully three M.Phil. and 28 Ph.D. students and made contributions in the area of receiver design to several European-funded research projects including long range telemetry in ultra-shallow channels, shallow water acoustic network, and acoustic communication network for the monitoring of the underwater environment in coastal areas for 12 years.

Jonathon Chambers (S'83–M'90–SM'98–F'11) received the Ph.D. and D.Sc. degrees in signal processing from the Imperial College of Science, Technology and Medicine, London, U.K., in 1990 and 2014, respectively. From 1991 to 1994, he was a Research Scientist with Schlumberger Cambridge Research, Cambridge, U.K. In 1994, he returned to Imperial College London as a Lecturer in signal processing and was promoted to Reader (Associate Professor) in 1998. From 2001 to 2004, he was the Director of the Center for Digital signal processing and a Professor of Signal Processing with the Division of Engineering, King's College London, where he is currently a Visiting Professor. From 2004 to 2007, he was a Cardiff Professorial Fellow with the School of Engineering, Cardiff University, Cardiff, U.K. From 2007 to 2014, he led the Advanced Signal Processing Group with the School of Electronic, Electrical and Systems Engineering, Loughborough University, U.K., where he is currently a Visiting Professor. In 2015, he joined the School of Electrical and Electronic Engineering, Newcastle University, where he is also a Professor of signal and information processing and heads the ComS2IP Group. He is also a Guest Professor with Harbin Engineering University. He has served as an Advisor to over 70 Ph.D. graduates and published over 500 outputs. He is a Fellow of the Royal Academy of Engineering, the Institution of Electrical Engineers, and the Institute of Mathematics in its Applications in the U.K. He has served as an Associate Editor of the IEEE TRANSACTIONS ON SIGNAL PROCESSING from 1997 to 1999, and from 2004 to 2007, and a Senior Area Editor from 2011 to 2015.